Quadratic Optimal Control Theory For Viscoelastically Damped Structures using a Fractional Derivative Viscoelasticity Model

THESIS

Richard N. Walker, B.S.
Captain, USAF

DEPARTMENT OF THE AIR FORCE
AIR UNIVERSITY
AIR FORCE INSTITUTE OF TECHNOLOGY

Wright-Patterson Air Force Base, Ohio

AFIT/GA/AA/88D-12

Quadratic Optimal Control Theory For Viscoelastically Damped Structures using a Fractional Derivative Viscoelasticity Model

THESIS

Richard N. Walker, B.S.
Captain, USAF

AFIT/GA/AA/88D-12

Approved for public release; distribution unlimited

AFIT/GA/AA/88D-12

QUADRATIC OPTIMAL CONTROL THEORY FOR VISCOELASTICALLY DAMPED STRUCTURES USING A FRACTIONAL DERIVATIVE VISCOELASTICITY MODEL

THESIS

Presented to the Faculty of the School of Engineering

of the Air force Institute of Technology

Air University

In Partial Fulfillment of the

Requirements for the Degree of

Master of Science in Astronautical Engineering

Richard N. Walker, B.S.

Captain, USAF

AFIT/GA/AA/88D-12

Acknowledgements

I would like to thank Lt Col Ronald Bagley, my thesis advisor, for his tireless and enthusiastic support of this project. He treated me more as a colleague than a student and through this association taught me much about research and myself. I hope that I may be fortunate enough to work with him again.

I would also like to thank the other members of my thesis committee, Dr. Robert Calico and Captain Greg Warhola, for their aid and insight to help me over the obstacles and to see meaning in the work. I would especially like to thank Capt Warhola for his toleration of my engineering mathematics and for his reminders that "you're in grad school now." I would especially like to thank him for "being there" to help bale me out of my last minute problems.

A friend not to be overlooked is my roommate, Capt Walter Jurek. A fellow AFIT student who suffered my moods and listened to my trials but always remained my friend. He was also fun to live with and constantly kept my spirits up. Who else but a true friend (or your paid typist) would help you type the eleventh corrections?

Finally, but actually first, I thank God for His inspiration and the courage and knowledge to complete this task.

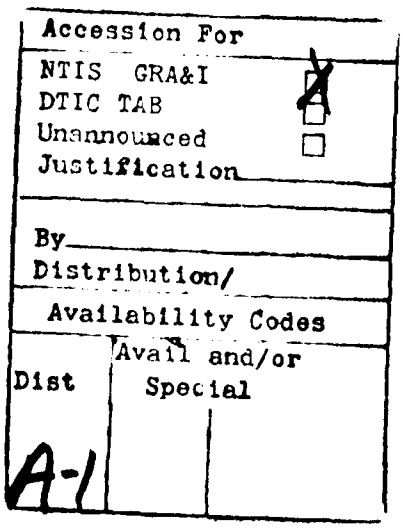

Richard N. Walker

Table of Contents

List of Figures

List of Tables

optimal gain matrix for large time for the fractional state-space system.

Unfortunately, in the general time case, no Riccati equation can be derived because of coupling between the optimal gain matrix and the state vector due to fractional derivatives of the control vector. Only when gain matrices are asymptotically constant for time large and time is large, do they uncouple.

The theory is illustrated by two examples. A simply-supported viscoelastic beam with controllers illustrates the solution process in Example 1. The beam example incorporates the fractional calculus viscoelastic behavior in a structure element, while an axially deforming rod in Example 2 incorporates the behavior through a viscoelastic shear force applied at a node by a damping pad. The example equations of motion are numerically solved using the commercially-available control analysis software package called MATRIX$_X$.

Abstract

The objective of this thesis is to develop a control law for structures incorporating both passive damping via viscoelastic materials modelled by a fractional calculus stress-strain law and active damping by applied forces and torques. To achieve this, quadratic optimal control theory is modified to accomodate systems with fractional derivatives in the state vector. Specifically, linear regulator theory is modified.

The approach requires expanding the structure's equation of motion into a fractional state-space system of order 1/n, where n is an integer based on the viscoelastic damping material constitutive law. This approach restricts the theory to materials which have rational, fractional derivatives in their constitutive laws. An equivalent first-order system is then formed and used to derive the optimal control theory in linear regulator problems. The quadratic performance index used in linear regulator theory is used, and equations similar to those derived for linear regulator problems using first-order systems are developed. The optimal control law is asymptotically linear feedback of the state vector for time large. An equation which defines the optimal gain matrix for the feedback is derived and is asymptotically an algebraic Riccati equation for long time and for gain matrices which are asymptotically constant for large time. Since an algebraic Riccati equation can be defined, current solving routines can determine the asymptotically constant

optimal gain matrix for large time for the fractional state-space system.

In the general time case, no Riccati equation can be derived because of coupling between the optimal gain matrix and the state vector due to fractional derivatives of the control vector. Only when time is large and gain matrices are asymptotically constant, do they uncouple .

The theory is illustrated by two examples. A simply-supported viscoelastic beam with controllers illustrates the solution process in Example 1. The beam example incorporates the fractional calculus viscoelastic behavior in a structure element, while an axially deforming rod in Example 2 incorporates the behavior through a viscoelastic shear force applied at a node by a damping pad. The example equations of motion are numerically solved using the commercially-available control analysis software package called MATRIX$_X$.

QUADRATIC OPTIMAL CONTROL THEORY FOR VISCOELASTICALLY DAMPED STRUCTURES USING A FRACTIONAL DERIVATIVE VISCOELASTICITY MODEL

I. Introduction

Control of large flexible structures is currently of interest because of, in part, the possible use of large space structures in the Strategic Defense Initiative. Fine pointing and position requirements drive the need for fast, accurate control of a structure's state. Primary emphasis in the past has been on purely elastic structures controlled by various applied forces and torques in feedback. Unfortunately, large flexible structures have large numbers of vibrational modes at low frequencies which are easy to excite. The modes are also very closely spaced in frequency, so that control of one often excites one or more other close modes. Thus, control accuracy is degraded. The incorporation of viscoelastic materials into structures holds promise to improve active control performance considerably.

One primary reason that viscoelastic materials have not been readily included is that classical models of viscoelastic behavior are complex. The classical stress-strain law uses a sum of integer order, ordinary derivatives to describe the weak frequency dependence of the viscoelastic behavior:

$$\sigma + \sum_{i=1}^{m} b_i \frac{\partial^i \sigma}{\partial t^i} = E\varepsilon + \sum_{j=1}^{p} a_j \frac{\partial^j \varepsilon}{\partial t^j}$$

where σ is stress, ε is strain, a_j and b_i are constants, and m and p are integers. More or less derivatives are employed to fine tune the model to the precision required. High precision requires a large number of derivatives, implying also a large number of parameters (a_j and b_i). The large number of derivatives also expands the state vector which must be observed and fed back for control. This resulting calculations with large matrices are not condusive to fast response systems.

An alternate viscoelastic model uses fractional derivatives of time describe the material response. The fractional derivative of g(t) of order α, where α is taken to be a real fraction, is defined as

$$\frac{d^\alpha g(t)}{dt^\alpha} = \frac{1}{\Gamma(1-\alpha)} \frac{d}{dt} \int_0^t \frac{g(t-\tau)}{\tau^\alpha} d\tau \quad , \quad 0 \le \alpha < 1 \qquad (1)$$

Its Laplace transform is $[sG(s)-g(t=0)]/s^{1-\alpha}$, where s is the Laplace variable and the capital letter indicates the Laplace transform of g(t). The fractional calculus model of the constitutive law is

$$\sigma + b \frac{\partial^\beta \sigma}{\partial t^\beta} = E\varepsilon + a \frac{\partial^\alpha \varepsilon}{\partial t^\alpha} \qquad (2)$$

For this thesis b is chosen to be equal to zero; and α = m/n, where m and n are integers. Such a model is commonly called a "power-law" constitutive model (5). Bagley and Torvik (3:918) have shown that this model is accurate over four or more decades in frequency for over 130 viscoelastic materials. The virtue of this model is that it

requires only four parameters. However, it too requires expanding the state vector to include fractional derivatives, but the fractional derivatives are lower order than those used in the classical model. The effects of noise and uncertainities are not as dramatically amplified through the lower order diferentiation. Consequently, the fractional calculus model appears to be a better choice to incorporate into a control law.

The objective of this thesis is to attempt to incorporate the fractional calculus viscoelastic model into optimal control theory, such that an optimal control law for an active controller, which is optimal in a sense to be described, can account for and complement passive damping. Current state-space optimal control theory uses a performance index to optimize. Indices with quadratic terms are commonly used because energy is described by the square of the velocity and displacement. This is quadratic control theory. A special case, linear regulator theory, assumes a quadratic form for the optimal value of the performance index, J, i.e. $J^* = 1/2\ \vec{x}^T \tilde{K} \vec{x}$, where $\vec{x}$ is the state vector, $\tilde{K}$ is a matrix of gains, and the asterisk indicates an optimal value. In this special case quadratic control theory produces optimal control as linear feedback of the state vector. Because the feedback is linear, the analysis and its implementation is relatively straightforward. Therefore, this work focuses on deriving the equations in the linear regulator theory for a system using fractional state-space.

The current linear regulator equations are derived by the application of a first-order state-space system of the form:

$$\dot{\vec{x}}(t) = \tilde{A}(t)\,\vec{x}(t) + \tilde{B}(t)\,\vec{u}(t) \qquad (3)$$

where

$\vec{x}(t)$ = state vector
$\dot{\vec{x}}(t)$ = first derivative of the state vector with respect to time
$\vec{u}(t)$ = vector of control forces and torques
$\tilde{A}(t)$, $\tilde{B}(t)$ = matrices of functions

The approach taken in this thesis is to formulate a first-order system which is based on an expanded equation of motion of a structure (3:921-922) and derive the equations for the linear regulator theory. The expanded equation of motion is developed from converting a structure's finite element model into a state-space system. A finite element model which includes viscoelastic materials described by a fractional calculus model will generate a state vector which includes both integer and fractional derivatives. The general form of a system created by expanding a structure's equation of motion is a system of fractional order less than one and is

$$D_t^{1/n}\,\vec{x}(t) = \tilde{A}(t)\,\vec{x}(t) + \tilde{B}(t)\,\vec{u}(t) \qquad (4)$$

where $D_t^{1/n}$ is a fractional differential operator of order 1/n operating on the state vector in which n is the positive denominator integer of the material's rational fraction in the fractional derivative model of the material's viscoelastic behavior. The state vector includes fractional derivatives. It is shown herein that this approach leads to a simple control law.

For clarity in this thesis the term "classical" will refer to use of a first-order system instead of a system of order 1/n. For example, the "classical" eigenvalue problem refers to the eigenvalue problem which uses a first-order system.

II. Background

In the last ten years there has been a lot of work on the fractional calculus model of viscoelasticity. Bagley and Torvik (1,2,3,4,15) have published a number of papers on the model's use and accuracy. Bagley's PhD dissertation (1) details the calculation of material response for structures using the fractional calculus model. His research shows that the model predicts both oscillatory and non-oscillatory relaxation motion for viscoelastic materials (1:92-104). This latter motion is due to the characteristic relaxation which deformed viscoelastic materials exhibit in returning to a less stressed state over time. For example, the internal structure of a rubber band which has been left stretched for a long time will slowly adjust, such that the stress is relieved. This has been observed to be closely modelled by power-law phenomenon over finite observation times (20:681). Furthermore, Bagley (3:918) has experimentally determined the model parameters for over 130 materials and has found the model accurate over four or more decades in frequency. In their 1985 paper (3:921-923) Bagley and Torvik also illustrated a method to convert a finite element equation of motion for a structure incorporating elements using a model of order α, where $\alpha = m/n$ (m, n = integers), into a fractional state-space system of order 1/n. This forms the basis for building the first-order system required to develop the control theory.

Thus far, Skaar, Michel, and Miller (24:348) and Hannsgen, Renardy, and Wheeler (12:32-34) have investigated system control using the fractional calculus model. Neither use optimal control theory to develop an optimal control law. Both assume feedback forms and analyze the effects. The former restrict the feedback control law to a fractional derivative of the same order as the constitutive law, $P_\sigma(\sigma)=P_\varepsilon(\varepsilon)$, where P_σ and P_ε are differential operators, $P_\sigma=1 + a\partial^\nu/\partial t^\nu$ and $P_\varepsilon=E + b\partial^\nu/\partial t^\nu$, E is Young's modulus, a, b, and ν are constants, and ν is a rational fraction. The work focuses on the use of the root locus technique to analyze the system response. They derived the transfer function in terms of a new parameter, h, which is defined in the Laplace domain by $h^2 = s^2P_\sigma(s)/P_\varepsilon(s)$, where s is the Laplace variable. The poles of the transfer function, therefore, are values of h instead of s, the Laplace variable, and, as such, cannot be used directly to find the response. The poles must be mapped back to values of s through the definition of h, before the response can be calculated. A similar situation arises in the application of the control theory developed in this thesis and is demonstrated in the example problems. Furthermore, Skaar also noted that general stability criteria can be defined in the complex h-plane, so that the poles could be used directly to assess general characteristics of the system stability. Specificly, Skaar maps the imaginary axis from the complex s-plane to the h-plane and proves that all poles must lie to the left of this mapped line to have a stable system. Similar criteria are shown in this thesis.

In the latter work referred to above, Hannsgen, Renardy, and Wheeler investigate the response of a viscoelastic torsional rod subjected to linear feedback of the angular displacement. In a special case, they use the fractional derivative model for the constitutive law of the rod. High and low modes of vibration experienced different effects as control gain varies from low to high for this constitutive law. Specifically, for low gains the low frequency modes are least damped; but, as gain increases, higher frequency modes become the least stable. Optimal gain is defined as that gain which makes the poles of the least stable mode most stable compared to other gain value least stable pole locations, i.e. stability is classified by the least stable mode's most-negative-real location over the range of gains investigated. They define optimum is when it is most stable. This is a performance index, which optimizes a predetermined control law instead of creating one.

III. Theory

Performance Index

Optimization requires some measure of performance to minimize or maximize. This performance index (PI) contains expressions which represent important system characteristics, e.g. kinetic energy, and which are written in terms of system and control law parameters. Furthermore, these expressions are weighted, so that their effect on the overall performance index can be varied to emphasize certain parameters to find some "best" combination.

To create a performance index one must identify the important system characteristics and their representations of the system of interest. For this thesis that system is a state-space system of order 1/n with constant, real coefficient matrices, $\tilde{A}$ and $\tilde{B}$

$$D_t^{1/n} \vec{x}(t) = \tilde{A}\, \vec{x}(t) + \tilde{B}\, \vec{u}(t) \tag{5}$$

where $\vec{x}(t)$ is the state vector, which includes both integer and fractional derivatives of position, and $\vec{u}(t)$ is the control vector. The matrices $\tilde{A}$ and $\tilde{B}$ must be constant and real, because the system represents a finite element model of a structure. The structure equation of motion has constant, real coefficients. When the equation is expanded into a state-space system, matrices $\tilde{A}$ and $\tilde{B}$ are formed using these constant, real coefficients.

Structures are normally characterized by the amount of energy which the configuration, including control inputs, stores at any point

of time. Consequently, a performance index based on energy would be appropriate. Current optimal linear control theory gives a starting point. Kirk (15:91) uses a general PI of the following form for first-order linear systems of continuous linear regulator problems:

$$J = \frac{1}{2}\vec{x}^T(t_f)\,\tilde{H}\vec{x}(t_f) + \frac{1}{2}\int_{t_o}^{t_f}(\vec{x}^T\tilde{Q}\vec{x} + \vec{u}^T\tilde{R}\,\vec{u})dt \tag{6}$$

where J is the performance index, $\vec{x}(t)$ is the state vector, $\vec{u}(t)$ is the control vector, and $\tilde{H}$, $\tilde{Q}$, and $\tilde{R}$ are real, symmetric weighting matrices, in which $\tilde{R}$ is positive definite and $\tilde{H}$ and $\tilde{Q}$ are positive semi-definite. Values of $\tilde{H}$, $\tilde{Q}$, and $\tilde{R}$ are chosen for an optimization; consequently, each set of weighting matrices defines an optimized value of the performance index, J. For this thesis $\tilde{H}$, $\tilde{Q}$, and $\tilde{R}$ are chosen to be constant matrices. Since the state vector contains both position and its first derivative, $1/2\ \vec{x}^T\tilde{Q}\vec{x}$ includes measures for both the strain and kinetic energies of the structure. Similarly, $1/2\ \vec{u}^T\tilde{R}\vec{u}$ is a measure of energy in the controller. The expression with $\tilde{H}$ merely represents the energy in the desired final state. Although the extra fractional states are now included in the system, the classical definitions of strain and kinetic energy are assumed to still be valid. Furthermore, the extra fractional states are not known to represent any energy storage system. That is, the structure stored energy is still described by kinetic and strain energies. Consequently, a quadratic performance index should still be suitable for optimizing the 1/nth-order system. Weighting

matrices $\tilde{H}$ and $\tilde{Q}$, however, must be chosen such that the fractional states have zero weight. This eliminates these states from the index.

For the problems of interest, a slightly modified form of this PI is desireable. For simplicity the transient solution of the state vector is not addressed, and only the steady-state solution is sought. Therefore, let time be large and let t_f tend to infinity. Furthermore, when the desired final state is static equilibrium of the structure, $1/2\ \vec{x}^T(t_f)\ \tilde{H}\ \vec{x}(t_f)$ is assumed to be equal to zero. Therefore, the actual performance index used herein to optimize fractional-order systems of the form of Eq (5) is

$$J = \frac{1}{2}\int_0^\infty (\vec{x}^T \tilde{Q} \vec{x} + \vec{u}^T \tilde{R}\ \vec{u})dt \tag{7}$$

Modified Hamilton-Jacobi-Bellman Equation and Optimal Control Law

Kirk (15:86-90) thoroughly discusses the optimization of his general PI, which is a more general form of the chosen performance index,

$$J(\vec{x}(t),\ t,\ \underset{t\le\tau\le t_f}{\vec{u}(\tau)}) = h(\vec{x}(t_f),\ t_f) + \int_t^{t_f} g(\vec{x}(\tau), \vec{u}(\tau), \tau)\ d\tau \tag{8}$$

for a general first-order system of the form

$$\dot{\vec{x}}(t) = \vec{a}(\vec{x}(t), \vec{u}(t),\ t)$$

If the 1/nth-order system can be posed as a first-order system, then the optimization process for our performance index has already been outlined by Kirk. The development can be followed, and equations

pertaining to the system of order 1/n can be found. The linear regulator problem is specificly followed because it uses the same performance index as has been chosen for this thesis and results in linear feeback of the state matrix. It will be shown that the modified control law will also be linear or asymptotically linear for steady-state ($t \rightarrow \infty$).

Once a structure has been built, the only way to affect its stability is through applying some control force or torque, $\vec{u}(t)$. The state vector, $\vec{x}(t)$, is just a statement of the location and motion of the structure's parts, i.e. it is a description of the state of the structure. The control $\vec{u}(t)$ is what is being implemented to cause a change in the state of the structure. It is also the quantity for which the physical control system is going to be designed. Therefore, the control law which minimizes the performance index is what is being sought. Consequently, the performance index is minimized with respect to the control, $\vec{u}(t)$. The PI is minimized, because the control objective is minimum structural motion and minimum energy used by the controllers, all of which is characterized by minimum energy in the system. The control $\vec{u}(t)$ which minimizes the index is designated the optimal control, $\vec{u}^*(t)$. The relation between $\vec{u}^*(t)$ and its variables (e.g. $\vec{x}(t)$ and t) is called the optimal control law. Therefore, the basic concept behind the development of this optimal control theory for systems of order 1/n is the determination of an optimal control law by minimization of the performance index with respect to the control, $\vec{u}(t)$:

$$J^*(\vec{x}(t),t) = \min_{\substack{\vec{u}(\tau) \\ t\le\tau\le t_f}} \left\{ h(\vec{x}(t_f),\, t_f) + \int_t^{t_f} g(\vec{x}(\tau), \vec{u}(\tau), \tau)\, d\tau \right\}$$

$$= h(\vec{x}(t_f),\, t_f) + \int_t^{t_f} g(\vec{x}(\tau), \vec{u}^*(\tau), \tau)\, d\tau \qquad (9)$$

where $J^*(\vec{x}(t),t)$ is the optimal performance index function. It is no longer a function of $\vec{u}(t)$, since the minimum over all admissible controls has been taken; i.e. J^* specifies $\vec{u}^*(t)$ as the optimal control.

Eq (9) defines $J^*(\vec{x}(t),t)$. However, the equation includes two unknown functions, because the optimal performance index function is unknown as well as the optimal control. There is, thus far, one equation for two unknowns; consequently, an expression for one of the unknowns must be assumed. A function is chosen for $J^*(\vec{x}(t),t)$ to emphasize system characteristics whcih are believed to be important, and the corresponding $\vec{u}^*(t)$ is found.

If, instead, the minimization is performed with $J^*(\vec{x}(t),t)$ unspecified, the optimal control will be a function of $J^*(\vec{x}(t),t)$, $\vec{x}(t)$, and t. Depending on its form, $J^*(\vec{x}(t),t)$ may have one or more constants of proportionality between itself and its variables; therefore, one or more equations are still necessary to completely describe the optimal control. If a simple form for the optimal index function is assumed, e.g. $J^*(\vec{x}(t),t) = 1/2\ \vec{x}^T\tilde{K}(t)\vec{x}$, then one equation for $\tilde{K}(t)$ and one for $\vec{u}^*(t)$, including $\tilde{K}(t)$ and $\vec{x}(t)$, are required. This is the case for the linear regulator problem. $\tilde{K}(t)$ is often called the optimal "gain" matrix, because it is the matrix of gains, i.e.

amplification factors applied to a feedback state, for the assumed optimal performance index function. Both equations are found through the minimization of the index as shown in the next section.

Kirk illustrates the optimization of a general performance index with the general first-order system, Eq (9). If there is an equivalent first-order system for the 1/nth-order system, it can be used the general equations that result from the optimization. Since the optimization is simple and Kirk (15:86-87) describes it well, it is not repeated here. Instead, this thesis will start from the resulting equation, the Hamilton-Jacobi-Bellman equation, and will detail the modification of the linear regulator theory equations for a system of order 1/n.

Modified Hamilton-Jacobi-Bellman Equation and Optimal Control Law

Kirk's development leads to the important Hamilton-Jacobi-Bellman (H-J-B) equation, which must be satisfied by the optimal PI, $J^*(\vec{x}(t), t)$:

$$0 = J_t^*(\vec{x}(t), t) + H(\vec{x}(t), \vec{u}^*(\vec{x}(t), \vec{J}_x^*, t), \vec{J}_x^*, t) \tag{10}$$

where the assumed final value is $J^*(\vec{x}(t_f), t_f) = 0$ and H, called the Hamiltonian, is

$$H(\vec{x}(t), \vec{u}(t), \vec{J}_x^*, t) = g(\vec{x}(t), \vec{u}(t), t) + \vec{J}_x^{*T}(\vec{x}(t), t)[\vec{a}(\vec{x}(t), \vec{u}(t), t)] \tag{11}$$

where $\vec{a}(\vec{x}(t), \vec{u}(t), t)$ is a first-order system. The Hamiltonian is minimized by the optimal control, $\vec{u}^*(t)$:

$$H\left(\vec{x}(t), \vec{u}^{*}(\vec{x}(t), \vec{J}_x^{*}, t), \vec{J}_x^{*}, t\right) = \min_{\vec{u}(t)} \left\{ H\left(\vec{x}(t), \vec{u}(t), \vec{J}_x^{*}, t\right) \right\} \tag{11a}$$

Eq(10) and Eq (11a) are important, because the minimization of the Hamiltonian yields the optimal control law and the H-J-B equation yields an equation for the optimal gain matrix in the performance index. Hence, these are the two equations sought in the previous section to describe the optimal control law.

The H-J-B equation is the relation that defines the general optimal performance index, $J^{*}(\vec{x}(t), t)$. However, as noted earlier, a form must be assumed for $J^{*}(\vec{x}(t), t)$, e.g. $1/2\ \vec{x}^{T}\ \tilde{K}(t)\ \vec{x}$ where $\tilde{K}(t)$ is the optimal gain matrix. If the PI is chosen appropriately, the H-J-B equation will give an equation for $\tilde{K}(t)$. Kirk pursues this approach. First, he minimizes the Hamiltonian with respect to a general J^{*} and finds that the optimal control law which minimizes it is given by linear feedback of the partial derivative of J^{*} with respect to $\vec{x}(t)$. Thus, the linear regulator problem is defined. If $J^{*}(\vec{x}(t), t)$ is chosen to be equal to $1/2\ \vec{x}^{T}\ \tilde{K}(t)\ \vec{x}$, the optimal control is linear feedback of the state vector. Using this optimal control and PI, the H-J-B equation leads to a nonlinear ordinary differential equation for the optimal gain matrix, $\tilde{K}(t)$. For the linear regulator problem this equation is a Riccati equation. If the 1/nth-order system could be posed as a first-order system, then a development parallel to Kirk's can be used to define modified versions of the H-J-B equation, optimal control law, and Riccati equation. Therefore, the problem reduces to writing the 1/nth-order system in the form of a first-

order system. Then substitute this expression and the index form, Eq (6), chosen for this thesis, into the general Riccati and Hamiltonian equations, and complete the minimization for this specific linear regulator problem.

The first-order system can simply be rewritten recursively in terms of the derivative of order 1/n which was defined in Eq (1):

$$\dot{\vec{x}} = D_t^{1/n}\left[D_t^{1/n} \cdots \left(D_t^{1/n}(\vec{x})\right)\right] \quad (n \text{ times}) \tag{12}$$

Successive replacement of $D_t^{1/n}\vec{x}$ by $\tilde{A}\,\vec{x}(t) + \tilde{B}\,\vec{u}(t)$, as in Eq (4), and application of the next derivative operator yields a general first-order system of the form:

$$\dot{\vec{x}} = \tilde{A}^n\vec{x} + \tilde{A}^{n-1}\tilde{B}\vec{u} + \tilde{A}^{n-2}\tilde{B}D_t^{1/n}\vec{u} + \tilde{A}^{n-3}\tilde{B}D_t^{2/n}\vec{u} + \cdots + \tilde{A}\tilde{B}D_t^{(n-2)/n}\vec{u} + \tilde{B}D_t^{(n-1)/n}\vec{u}$$

$$\boxed{\dot{\vec{x}} = \tilde{A}^n\vec{x} + \sum_{p=0}^{n-1}\tilde{A}^{n-p-1}\tilde{B}D_t^{p/n}\vec{u}} \tag{13}$$

where $D_t^0\,u(t) = u(t)$. This is illustrated by an example of a 1/3-order system with constant matrices $\tilde{A}$ and $\tilde{B}$:

$$\begin{aligned}
\dot{\vec{x}} &= D_t^{1/3}\left[D_t^{1/3}\left(D_t^{1/3}(\vec{x})\right)\right] \\
\dot{\vec{x}} &= D_t^{1/3}\left[D_t^{1/3}\left(\tilde{A}\,\vec{x}(t) + \tilde{B}\,\vec{u}(t)\right)\right] \\
\dot{\vec{x}} &= D_t^{1/3}\left[\tilde{A}\,D_t^{1/3}\vec{x}(t) + \tilde{B}\,D_t^{1/3}\vec{u}(t)\right] \\
\dot{\vec{x}} &= D_t^{1/3}\left[\tilde{A}\left(\tilde{A}\,\vec{x}(t) + \tilde{B}\,\vec{u}(t)\right) + \tilde{B}\,D_t^{1/3}\vec{u}(t)\right]
\end{aligned} \tag{14.a-g}$$

$$\dot{\vec{x}} = \tilde{A}^2 D_t^{1/3} \vec{x}(t) + \tilde{A}\tilde{B} D_t^{1/3} \vec{u}(t) + \tilde{B} D_t^{2/3} \vec{u}(t)$$

$$\dot{\vec{x}} = \tilde{A}^2 \left(\tilde{A} \vec{x}(t) + \tilde{B} \vec{u}(t) \right) + \tilde{A}\tilde{B} D_t^{1/3} \vec{u}(t) + \tilde{B} D_t^{2/3} \vec{u}(t)$$

$$\dot{\vec{x}} = \tilde{A}^3 \vec{x}(t) + \tilde{A}^2 \tilde{B} \vec{u}(t) + \tilde{A}\tilde{B} D_t^{1/3} \vec{u}(t) + \tilde{B} D_t^{2/3} \vec{u}(t)$$

The resulting expression can be used with the H-J-B equation to develop the optimal control law and a modified Riccati equation governing the gain $\tilde{K}(t)$ in the 1/nth order system. An important point is that this development is restricted to systems of rational 1/nth-order since n must be an integer to apply the derivative n times in the recursive relation for $\dot{\vec{x}}$.

The first step in using this equivalent form in the H-J-B equation is minimization of the Hamiltonian with respect to the control vector; a necessary condition is vanishing of the first variation: $\frac{\partial H}{\partial \vec{u}} = 0$. If the second variation, $\frac{\partial^2 H}{\partial \vec{u}^2}$, is a positive-definite quadratic form, the control vector which solves this is the desired optimal control vector. The minimum value of H is found by evaluating it at the optimal control vector.

Using the equivalent first-order system, Eq (13), the Hamiltonian becomes

$$H = \frac{1}{2} \vec{x}^T \tilde{Q} \vec{x} + \frac{1}{2} \vec{u}^T \tilde{R} \vec{u} + \vec{J}_x^{*T} \left(\tilde{A}^n \vec{x} + \sum_{p=0}^{n-1} \tilde{A}^{n-p-1} \tilde{B} D_t^{p/n} \vec{u} \right) \qquad (15)$$

To find the first variation with respect to $\vec{u}$, evaluate H at $\vec{u} + \vec{h}$:

$$H = \frac{1}{2}\vec{x}^T\tilde{Q}\vec{x} + \frac{1}{2}(\vec{u}+\vec{h})^T\tilde{R}(\vec{u}+\vec{h}) + \vec{J}_x^{*T}\left(\tilde{A}^n\vec{x} + \sum_{p=0}^{n-1}\tilde{A}^{n-p-1}\tilde{B}D_t^{p/n}(\vec{u}+\vec{h})\right)$$

Simplify, using $\frac{1}{2}\vec{h}^T\tilde{R}\vec{u} = \frac{1}{2}\vec{u}^T\tilde{R}\vec{h}$ (which is a scalar); the result is

$$H = H(\vec{u}) + \frac{\partial H}{\partial \vec{u}}(\vec{h}) + \frac{\partial^2 H}{\partial \vec{u}^2}(\vec{h}) \tag{16a}$$

where

$$H(\vec{u}) = \frac{1}{2}\vec{x}^T\tilde{Q}\vec{x} + \frac{1}{2}\vec{u}^T\tilde{R}\vec{u} + \vec{J}_x^{*T}\left(\tilde{A}^n\vec{x} + \sum_{p=0}^{n-1}\tilde{A}^{n-p-1}\tilde{B}D_t^{p/n}\vec{u}\right) \tag{16b}$$

$$\frac{\partial H}{\partial \vec{u}}(\vec{h}) = \vec{u}^T\tilde{R}\vec{h} + \vec{J}_x^{*T}\sum_{p=0}^{n-1}\tilde{A}^{n-p-1}\tilde{B}D_t^{p/n}\vec{h} \tag{16c}$$

$$\frac{\partial^2 H}{\partial \vec{u}^2}(\vec{h}) = \frac{1}{2}\vec{h}^T\tilde{R}\vec{h} \tag{16d}$$

This is an the expansion of H evaluated at $\vec{u}+\vec{h}$. The first variation, or derivative, of H operating on $\vec{h}$ corresponds to the terms linear in $\vec{h}$. The second variation corresponds to the terms quadratic in $\vec{h}$. With the requirement that $\tilde{R}$ be positive definite, the second variation is always positive. Therefore, a solution of the first variation will give a minimum value.

The first variation, Eq (16c), operating on $\vec{h}$ must equal zero for any admissible $\vec{h}$,

$$\vec{u}^T \tilde{R} \vec{h} + \vec{J}_x^{*T} \sum_{p=0}^{n-1} \tilde{A}^{n-p-1} \tilde{B} D_t^{p/n} \vec{h} = 0 \qquad (17)$$

where admissible controls and variations are taken to be functions $\vec{h}(t)$ which are continuous for $0 \le t < \infty$. Since Eq (17) must be true for all admissible variations, $\vec{h}(t)$, it must, in particular, be true for the admissible variation

$$\vec{h}(t) = H(t)\,\vec{1} \qquad (18)$$

where H(t) is the Heaviside step function which is zero for $t < 0$ and 1 for $t > 0$; the vector $\vec{1}$ is the constant vector having the value 1 for all components. For this admissible variation, the fractional derivative is

$$D_t^{p/n} \vec{h}(t) = D_t^{p/n} H(t)\,\vec{1} = \frac{1}{\Gamma(1-p/n)} \frac{d}{dt} \int_0^t H(t-\tau)\,\tau^{-p/n}\,d\tau\,\vec{1} \qquad (19)$$

which yields

$$D_t^{p/n} \vec{h}(t) = T_{pn}(t)\,\vec{1} \qquad (20)$$

where

$$T_{pn}(t) = \begin{cases} 0, & t \le 0 \\ 1, & p = 0,\ t > 0 \\ \dfrac{t^{-p/n}}{\Gamma(1-p/n)}, & p > 0,\ t > 0 \end{cases} \qquad (21)$$

Using Eq (20) in Eq (17), the optimal control $\vec{u}^*$ must be

$$\vec{u}^*(t) = -\tilde{R}^{-1} \sum_{p=0}^{n-1} \tilde{B}^T \left(\tilde{A}^{n-p-1}\right)^T T_{pn}(t)\, \vec{J}_x^*(\vec{x}(t), t) \tag{22}$$

Observe that the large-time behavior of $\vec{u}^*$ is

$$\vec{u}^*(t) \sim -\tilde{R}^{-1} \tilde{B}^T \left(\tilde{A}^{n-1}\right)^T \vec{J}_x^*(\vec{x}(t), t) \quad , t \to \infty \tag{23}$$

The small-time form of $\vec{u}^*$ includes singular factors through $T_{pn}(t)$ which must be dominated by appropriate behavior of $\vec{J}_x^*$ for small values of t, in order for $\vec{u}^*$ to be an admissible control. This constraint on J will appear in initial conditions on the gains $\tilde{K}$ obtained from a Riccati equation.

The Riccati Equation for the Gains

The goal of this section is to derive the Riccati equation which governs, for large time, the gain matrix, $\tilde{K}(t)$, for linear regulator problems in which gains are asymptotically constant. Upon choosing an appropriate form for the optimal PI and applying it to the control law, Eq (22), the Riccati equation is derived with an application of the H-J-B equation. Using Eq (16b) in Eq (9), the H-J-B equation is now

$$0 = J_t^* + \frac{1}{2}\vec{x}^T\tilde{Q}\vec{x} + \frac{1}{2}\vec{u}^{*T}\tilde{R}\vec{u}^* + \vec{J}_x^{*T}\left(\tilde{A}^n\vec{x} + \sum_{p=0}^{n-1}\tilde{A}^{n-p-1}\tilde{B}D_t^{p/n}\vec{u}^*\right) \tag{24}$$

Recall, linear state feedback is achieved if J^* is quadratic in $\vec{x}$. Furthermore, it is logical that the PI may be related to the

expressions representing the system characteristics of interest. Therefore, it is commonly assumed that the PI takes the form

$$J^*(\vec{x}(t), t) = \frac{1}{2}\vec{x}^T \tilde{K}(t)\,\vec{x} \tag{25}$$

where $\tilde{K}(t)$ is real, symmetric, and positive-definite. Then

$$\vec{J}_x^* = \tilde{K}\vec{x} \tag{26}$$

and

$$J_t^* = \frac{1}{2}\vec{x}^T\dot{\tilde{K}}\vec{x} \tag{27}$$

Using Eq (26) in Eq (22), the optimal control law becomes

$$\vec{u}^*(t) = -\tilde{R}^{-1}\sum_{p=0}^{n-1}\tilde{B}^T\left(\tilde{A}^{n-p-1}\right)^T T_{pn}(t)\,\tilde{K}(t)\,\vec{x}(t) \tag{28}$$

(From this result, the large-time behavior of $\vec{u}^*$ can be viewed in terms of the behavior of $\vec{x}$, since $\tilde{K}$ is asymptotically constant. Furthermore, the initial behavior of $\tilde{K}$ can be ascertained to dominate the singular nature of $T_{pn}(t)$.)

When Eq (27) and the optimal control, $\vec{u}^*$, in Eq (28) are inserted into the H-J-B equation, Eq (24), the result after simplification is

$$\frac{1}{2}\vec{x}^T\left\{\dot{\tilde{K}} + \tilde{Q} + \tilde{K}\sum_{p=0}^{n-1}\tilde{A}^{n-p-1}\tilde{B}T_{pn}(t)\,\tilde{R}^{-1}\tilde{B}^T\sum_{q=0}^{n-1}\left(\tilde{A}^{n-q-1}\right)^T T_{qn}(t)\,\tilde{K} + 2\tilde{K}\tilde{A}^n\right\}\vec{x}$$

$$= \frac{1}{2}\vec{x}^T 2\tilde{K} \sum_{p=0}^{n-1} \tilde{A}^{n-p-1}\tilde{B}\, D_t^{p/n}\left[\sum_{q=0}^{n-1} \tilde{R}^{-1}\tilde{B}^T\left(\tilde{A}^{n-q-1}\right)^T T_{qn}(t)\, \tilde{K}(t)\, \vec{x}(t)\right] \tag{29}$$

At this point, we note that a commonly-employed technique saying "if $\vec{x}^T\tilde{M}\vec{x} = 0$ for any $\vec{x}$, then $\tilde{M} = 0$" cannot be used since the differential operator $D_t^{p/n}$ operates on both $\vec{x}$ and $\tilde{K}$; they cannot be separated in Eq (29) to use this argument to get an equation which $\tilde{K}$ must satisfy. However, consideration of the individual terms summed over p in the right side of Eq (29) reveals that, for gains $\tilde{K}$ which are asymptotically constant for large time, there are states, $\vec{x}(t)$, for which the leading order behavior of this sum is given by its p=0 term. In effect, the fractional derivatives of order greater than zero are subdominant to the undifferentiated (p=0) summation over q. Relying on "regularly-varying" function theory (Appendix A), Warhola (27) illustrates states for which this is true, so that the theory presented hereafter is not empty. Proceeding with this Eq (29) yields

$$\frac{1}{2}\vec{x}^T\left\{\dot{\tilde{K}}+\tilde{Q}+\tilde{K}\sum_{p=0}^{n-1}\tilde{A}^{n-p-1}\tilde{B}T_{pn}(t)\,\tilde{R}^{-1}\tilde{B}^T\sum_{q=0}^{n-1}\left(\tilde{A}^{n-q-1}\right)^T T_{qn}(t)\,\tilde{K}+2\tilde{K}\tilde{A}^n\right\}\vec{x}$$

$$\sim\ \frac{1}{2}\vec{x}^T 2\tilde{K}\,\tilde{A}^{n-1}\tilde{B}\sum_{q=0}^{n-1}\tilde{R}^{-1}\tilde{B}^T\left(\tilde{A}^{n-q-1}\right)^T T_{qn}(t)\,\tilde{K}\vec{x}\quad,\ t\to\infty \tag{30}$$

The leading order of the sum over q is clearly the zeroth term, so

$$\frac{1}{2}\vec{x}^T\left\{\dot{\tilde{K}}+\tilde{Q}+\tilde{K}\sum_{p=0}^{n-1}\tilde{A}^{n-p-1}\tilde{B}T_{pn}(t)\,\tilde{R}^{-1}\tilde{B}^T\sum_{q=0}^{n-1}\left(\tilde{A}^{n-q-1}\right)^T T_{qn}(t)\,\tilde{K}+2\tilde{K}\tilde{A}^n\right\}\vec{x}$$

$$\sim\ \frac{1}{2}\vec{x}^T 2\tilde{K}\,\tilde{A}^{n-1}\tilde{B}\;\tilde{R}^{-1}\tilde{B}^T\left(\tilde{A}^{n-1}\right)^T\tilde{K}\vec{x}\quad,\ t\to\infty \tag{31}$$

Now this must be true for all states, $\vec{x}(t)$, so

$$\dot{\tilde{K}}+\tilde{Q}+\tilde{K}\sum_{p=0}^{n-1}\tilde{A}^{n-p-1}\tilde{B}T_{pn}(t)\,\tilde{R}^{-1}\tilde{B}^T\sum_{q=0}^{n-1}\left(\tilde{A}^{n-q-1}\right)^T T_{qn}(t)\,\tilde{K}+2\tilde{K}\tilde{A}^n$$

$$\sim\ 2\tilde{K}\,\tilde{A}^{n-1}\tilde{B}\;\tilde{R}^{-1}\tilde{B}^T\left(\tilde{A}^{n-1}\right)^T\tilde{K}\quad,\ t\to\infty \tag{32}$$

Similar examination of the terms in the left side of Eq (32) reveals that the p=q=0 term dominates for large time, at least for asymptotically constant gains, $\tilde{K}$, which have a regularly-varying derivative, $\dot{\tilde{K}}$. (In fact, the $\dot{\tilde{K}}$ term is subdominant to all terms with p+q < n on the left side of Eq (32).) Thus,

$$\tilde{Q} + \tilde{K}\tilde{A}^{n-1}\tilde{B}\tilde{R}^{-1}\tilde{B}^{T}\left(\tilde{A}^{n-1}\right)^{T}\tilde{K} + 2\tilde{K}\tilde{A}^{n}$$

$$\sim 2\tilde{K}\tilde{A}^{n-1}\tilde{B}\ \tilde{R}^{-1}\tilde{B}^{T}\left(\tilde{A}^{n-1}\right)^{T}\tilde{K}\quad , t \to \infty \tag{33}$$

In the limit as $t \to \infty$, the algebraic Riccati equation governing the steady-state gains, $\tilde{K}$, is obtained as

$$\tilde{Q} + 2\tilde{K}\tilde{A}^{n} - \tilde{K}\tilde{A}^{n-1}\tilde{B}\tilde{R}^{-1}\tilde{B}^{T}\left(\tilde{A}^{n-1}\right)^{T}\tilde{K} = 0 \tag{34}$$

Now, the matrix $\tilde{K}\tilde{A}^{n}$ can be split into its symmetric and anti-symmetric parts

$$\tilde{K}\tilde{A}^{n} = \frac{1}{2}\left[\tilde{K}\tilde{A}^{n} + \left(\tilde{K}\tilde{A}^{n}\right)^{T}\right] + \frac{1}{2}\left[\tilde{K}\tilde{A}^{n} - \left(\tilde{K}\tilde{A}^{n}\right)^{T}\right]$$

Using the fact that the transpose of a scalar is itself, i.e.

$$\vec{x}^{T}\,\tilde{K}\tilde{A}^{n}\,\vec{x} = \vec{x}^{T}\left(\tilde{K}\tilde{A}^{n}\right)^{T}\vec{x}$$

then $2\tilde{K}\tilde{A}^{n}$ can be written as

$$2\tilde{K}\tilde{A}^{n} = \tilde{K}\tilde{A}^{n} + \left(\tilde{K}\tilde{A}^{n}\right)^{T}$$

Substituting Eq (35) into Eq (34) and, again, using the fact that the transpose of a scalar is itself, the result is the final form for the algebraic Riccati equation governing the limit of steady-state (asymptotically constant) gains, $\tilde{K}$, for a system of order1/n

$$\boxed{0 = \tilde{Q} + \tilde{K}\tilde{A}^{n} + \left(\tilde{K}\tilde{A}^{n}\right)^{T} - \tilde{K}\tilde{A}^{n-1}\tilde{B}\tilde{R}^{-1}\tilde{B}^{T}\left(\tilde{A}^{n-1}\right)^{T}\tilde{K}} \tag{36}$$

It is important to note that the constant-K Riccati equation for first-order systems is

$$0 = \dot{\tilde{K}} + \tilde{Q} + \tilde{K}\tilde{A}_1 + (\tilde{K}\tilde{A}_1)^T - \tilde{K}\tilde{B}_1\tilde{R}^{-1}\tilde{B}_1^T\tilde{K} \tag{37}$$

where

$$\dot{\vec{x}}(t) = \tilde{A}_1\,\vec{x}(t) + \tilde{B}_1\,\vec{u}(t) \tag{38}$$

Consequently, the modified 1/nth-order system equation can be written as an equivalent first-order system equation, if

$$\tilde{A}_1 = \tilde{A}^n \tag{39}$$

$$\tilde{B}_1 = \tilde{A}^{n-1}\tilde{B}. \tag{40}$$

The significance of this result is that current algebraic Riccati equation solving routines for first-order systems can be used to solve the modified, constant-K, steady-state equation for 1/nth-order systems. The tools to do this analysis are already available and in common use.

Solution Process for System Response

Once $\tilde{K}$ has been found by solving the Riccati equation (36), the solution for the state vector, $\vec{x}(t)$, can be completed. This solution is typically called the response of a system, because the state vector describes how a structure reponds to a given input. By substitution of the steady-state optimal control expression, Eq (29), into the system of order 1/n, Eq (5), the steady-state system equation becomes

$$D_t^{1/n}\vec{x} = \left[\tilde{A} - \tilde{R}^{-1}\tilde{B}^T\left(\tilde{A}^{n-1}\right)^T\tilde{K} \right]\vec{x} \qquad (41a)$$

The Laplace transform of Eq (41a), assuming zero initial conditions, is

$$s^{1/n}\vec{X}(s) = \left[\tilde{A} - \tilde{R}^{-1}\tilde{B}^T\left(\tilde{A}^{n-1}\right)^T\tilde{K} \right]\vec{X}(s) \qquad (41b)$$

where s is the Laplace variable and capital letters on the vectors indicate transforms. In the structure examples, the state vector is actually a composite of fractional order derivatives of displacement vectors, e.g.

$$\vec{x} = \begin{Bmatrix} D_t^{3/2}\{x\} \\ D_t^{1}\{x\} \\ D_t^{1/2}\{x\} \\ D_t^{0}\{x\} \end{Bmatrix}$$

where {x} is a vector of displacements. The solution technique is discussed next in general terms and is illustrated in detail in the example problems in Chapter 4.

If the system eigenvalues, λ, are defined by $\lambda = s^{1/n}$, then the solution process is reduced to an eigenvalue problem, i.e. $\lambda\vec{x} = \tilde{C}\vec{x}$, where $\tilde{C}$ is a real matrix for structures:

$$\lambda\vec{X}(s) = \left[\tilde{A} - \tilde{R}^{-1}\tilde{B}^{T}\left(\tilde{A}^{n-1}\right)^{T}\tilde{K} \right]\vec{X}(s) \qquad (42)$$

Insight to solving Eq (42) for the state vector response can be gained by reviewing the eigenvalue problem of a first-order system.

In the classical first-order system eigenvalue problem eigenvalues are defined in the Laplace domain by the relation $\omega = s$, which results in the solution of the state vector as $\vec{x} = \vec{\phi}\, e^{\omega t}$, where $\vec{\phi}$ is a vector of coefficents and ω is a complex number. The vector $\vec{\phi}$ is called an eigenvector, and each eigenvalue defines one. The complex plane in which the eigenvalues lie will be called the s^1-plane, where the superscript indicates the power of the Laplace variable s in the definition of the eigenvalue. If Eq (42) were an eigenvalue problem of a first-order system, by substitution of the transform of the general solution of the state vector, Eq (42) can be written as

$$0 = \left[\tilde{A} - \tilde{R}^{-1}\tilde{B}^{T}\left(\tilde{A}^{n-1}\right)^{T}\tilde{K} - \lambda\tilde{I} \right]\vec{\phi} \qquad (43)$$

where $\tilde{I}$ is the identity matrix. If the eigenvector is not the trivial solution, Eq (43) has a solution if and only if the determinant of the matrix of coefficents of the eigenvector is zero (18:78).

$$0 = \left| \tilde{A} - \tilde{R}^{-1}\tilde{B}^{T}\left(\tilde{A}^{n-1}\right)^{T}\tilde{K} - \lambda\tilde{I} \right| \tag{44}$$

Eq (44) yields a polynomial equation in the eigenvalue λ, and the roots of this polynomial are the eigenvalues. Because all coefficients of the polynomial are real, the eigenvalues may include real values or pairs of complex conjugate numbers. Once the eigenvalues are determined, the eigenvectors, $\vec{\phi}$, can be determined from Eq (43). The vectors are unique in that the ratio between any two elements is constant, but the values are not unique (18:78). The ratio is dependent on the eigenvalue, but the values are arbitrary because $c\vec{\phi}$, where c is an arbitrary constant, is also a solution of Eq (43). In typical equations of motion for structures $\vec{x}$, hence $\vec{\phi}$, are displacements. Since only the ratio of elements in the eigenvector is constant, the eigenvector represents relative displacements between nodal ponts in the structure. If the eigenvector is real valued, this gives a shape of the structure. Consequently, the eigenvector is called a mode shape, i.e. the shape of a mode of motion. These modes are quantized in that they only occur in conjunction with specific eigenvalues. It can be shown that the eigenvalues correspond to frequencies of vibration, if the motion is oscillatory (complex eigenvalue), or reciprocals of time constants, if the motion is non-oscillatory (real eigenvalues) (18:78).

Therefore, structures may vibrate in a specific shape at one of these "natural" frequencies or have a specific shape as the motion decays or grows with a specific time constant. Modes are named by the type of motion and eigenvalue ranking, when eigenvalues are ordered starting with the lowest value for that type, e.g. the second vibrational mode corresponds to the next eigenvalue higher than the lowest vibrational eigenvalue. If the eigenvector is complex, the mode shape changes as time passes. Finally, the total structural response may be expressed as a linear combination of responses due to individual modes (19:164). The lowest modes have the greatest influence because displacements, hence energy, are greater than the higher numbered modes. Once eigenvalues and eigenvectors are known in the classical eigenvalue problem, one can go directly to response.

Consequently, eigenvalues, called poles in control analysis, and eigenvectors are typically the focus in structural and control analysis. Because the pole affects the exponent of the exponential in the solution, $\vec{x} = \vec{\phi}\, e^{\omega t}$, its value determines stability, i.e. bounded motion, of the response. If ω is complex, the exponential can be written as a product of two exponentials: one with a real exponent and one with an imaginary exponent. The Euler formula (17:584) states that the latter can be written in terms of a real cosine part and an imaginary sine part. Therefore, a complex pole produces oscillatory response, in which the magnitude of the imaginary coefficient of time, t, in the exponent is the frequency of oscillation. Oscillatory motion is bounded, so it is the real

component of the pole which must determine the boundedness of motion. If the real part is positive, its exponential, which is the amplitude of the oscillatory motion, grows without bound. If the real part is negative or zero, the response is bounded, and the system is stable. Therefore, pole location can give a general idea of the response of the function, e.g. a pole in the second quadrant is stable and produces oscillatory motion, and is a primary tool in analysis of structural motion and control. The criteria that non-positive real parts of poles produce bounded motion only applies when the poles are expressed in this plane. Other criteria will be derived for eigenvalues expressed in other planes.

For systems of order 1/n, the eigenvalue is defined herein by $\lambda = s^{1/n}$, where λ is the eigenvalue and the eigenvalues lie on a complex plane called the $s^{1/n}$-plane. The general form of the time-domain state vector response is no longer the exponential; it is something more complex. A solution to Eq (42) can still be found relatively easily by mapping the eigenvalues for the system of order 1/n to a first-order system. Recalling the recursive equation for an equivalent first-order system, Eq (12), one can determine that for an eigenvalue, λ, which is defined by first-order system, $\lambda = \omega^n$. This implies two important ideas. First, one can determine the eigenvalues, λ, map them to ω, and determine system response from ω as described for the classical system. Second, because the eigenvalue λ is the nth-root of the eigenvalue ω, there are n λ-eigenvalues corresponding to a single ω-eigenvalue. These λ-poles actually produce more than just the response described by the

ω–eigenvalue. Some of the λ-poles produce the exponential response desribed by a corresponding ω–eigenvalue, but the others have been shown to generate terms of negative powers of time in the response (1:92-104). This power response corresponds to the relaxation or creep response observed by Nutting in viscoelastic materials (2:746, 20:681). If the equations of motion for the system of order 1/n are transformed into the Laplace domain, the complex plane will be called herein the $s^{1/n}$-plane, where the superscript denotes the order of the derivative in the eigenvalue definition.

The type of response due to a pole in the $s^{1/n}$-plane can be determined from pole location, just as in the s^1-plane. Because the λ-poles will be mapped into the s^1-plane to determine response, it is important to recognize which regions of the $s^{1/n}$-plane map to the four quadrants of the s^1-plane (Figure 1).

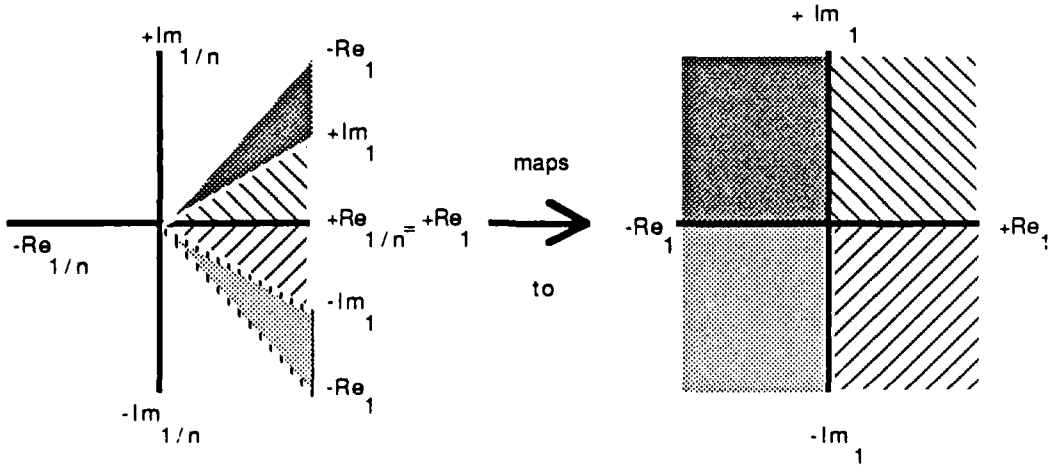

s^1-plane in $s^{1/n}$-plane s^1-plane

Figure 1. Mapping Regions Between $s^{1/n}$-plane and s^1-plane

The type of response due to poles in these regions of the $s^{1/n}$-plane is determined by the type in the corresponding s^1-plane quadrant. Poles will also lie outside these regions, and it has been shown that these poles produce relaxation response described by the terms of negative powers of time (1:92-104). The next section addresses poles and mapping in more detail.

Mapping Regions

Starting from the $s^{1/n}$-plane and mapping to the s^1-plane, the mapping function is

$$z_1 = (z_{1/n})^n \quad \text{where } z_{1/n} = \text{complex number in } s^{1/n}\text{-plane}$$

$$z_1 = \textit{complex number in } s^1\textit{-plane}$$

If one considers the inverse mapping, i.e. $z_{1/n}=(z_1)^{1/n}$, it is evident that each quadrant of the s^1-plane maps to a region of less angular width in the $s^{1/n}$-plane. The kth quadrant, $(k-1)\pi/2 \le \arg(z_1) < k\pi/2$ for k=1 to 4, maps to the smaller sector $(k-1)\pi/2n \le \arg(z_1) < k\pi/2n$. It is easy to identify which sectors of the $s^{1/n}$-plane map to each of the quadrants in the s^1-plane. The rays in the $s^{1/n}$-plane and the s^1-plane axes, to which they correspond (or map), bound the sectors in their respective plane:

$s^{1/n}$-plane		s^1-plane
The ray on which $s^{1/n} = A^{1/n} e^{i0}$	maps to $\rightarrow$	+ real axis
The ray on which $s^{1/n} = A^{1/n} e^{\pm i\pi/n}$	maps to $\rightarrow$	- real axis
The ray on which $s^{1/n} = A^{1/n} e^{i\pi/2n}$	maps to $\rightarrow$	+ imaginary axis
The ray on which $s^{1/n} = A^{1/n} e^{-i\pi/2n}$	maps to $\rightarrow$	- imaginary axis

where A is an arbitrary magnitude. This mapping is shown graphically in Figure 1. It is important to recognize that regions do not reduce or increase in size. The regions just appear differently on the two planes. The $s^{1/n}$-plane view only shows more regions so that the relaxation response can also be seen.

To understand to what these other regions refer, it is necessary to discuss the concept of a Riemann surface and sheets of complex numbers (17:621). Complex numbers be considered as on a spiral surface like an infinite corkscrew, because the angular parameter of a complex number is not unique. The angle is the same if $2\pi p$ radians, where p is an integer, are added or subtracted. Each complete twist of the screw represents one cycle of 2π radians. This twist is a sheet, often called a Riemann sheet, of complex numbers. Where the sheet begins and ends depends on the branch cut, which is defined by the specific problem and function singularities, in the plane. For example, since in this thesis the branch cut is assumed along the negative real axis, a sheet may be defined by those complex numbers whose argument (angle) lies between π and

$-\pi$. An analytic complex function requires a closed Riemann surface in order to satisfy the requirement of differentiability everywhere. The surface is composed of sheets joined together at the branch cuts, such that a continuous surface is formed. Because the function $w = z^n$ maps one sheet to n sheets, i.e. numbers with argument 2π become numbers with argument $2n\pi$, the corresponding Riemann surface consists of n sheets linked together at the branch cuts like a chain. The first and last cuts join to make a continuous surface, like a loop of chain.

In the classical first-order system eigenvalue problem in which the eigenvalue, λ, is defined by $D_t^1 \vec{x} = \lambda \vec{x}$ and there are no fractional powers of λ, the mapping function is $w = z^1$, and there is only one sheet. Hence, the reader may not be familiar with poles on other Riemann sheets. Once the eigenvalue problem is defined by $D_t^{1/n} \vec{x} = \lambda \vec{x}$, there are n sheets on whichthere are have poles; the $s^{1/n}$-plane view shows them all as sectors of angular width $2\pi/n$ radians. Considering the sheets as a stack, it is easy to visualize the plane representation as the projection of all the poles in the stack onto a planar surface. Often, because one is interested in poles on only one sheet, the mapping is applied to only those poles, and the poles are represented alone on a plane. This plane really only corresponds to the one sheet, but such a representation removes confusion concerning other poles of no current interest. Hence, this is done in this thesis. An example is the mapping in Figure 1.

The systems in the example problems which follow are of order one half and, thus, require surfaces of two sheets. One sheet is taken as

$$S_0 = \{ z \mid -\pi \leq \arg(z) < \pi \}$$

In order to avoid the confusion of jump discontinuities experienced by poles moving across the branch cut joining cuts defined at the extremes of the arg(z) range, e.g. 0 and 4π , this thesis uses two half-sheets:

$$S_{-1} = \{ z \mid -2\pi \leq \arg(z) < -\pi \}$$

$$S_1 = \{ z \mid \pi \leq \arg(z) < 2\pi \}$$

S_{-1} and S_1 are joined at $\arg(z)=2\pi$ and $\arg(z)= -2\pi$. S_{-1} is joined to S_0 at the branch cut where $\arg(z) = -\pi$, and S_1 is joined to S_0 at the branch cut where $\arg(z) = \pi$. The advantage of this choice of sheets is that mapping to the s^1-plane is done by halving the argument of the quantity being mapped and no poles move across the branch cut joining the extreme argument values. Consequently, the jump discontinuities in the argument are avoided. In summary, the poles lying in the $s^{1/n}$-plane outside the sectors corresponding to the S_0 Riemann sheet, considered the s^1-plane in this thesis, reside on other Riemann sheets. These poles have been shown to contribute terms of negative powers of time to the response (1:92-104), and these terms appear to correspond to creep or relaxation response in viscoelastic materials (2:748, 20:681). As such, this response is stable and non-oscillatory. Therefore, the poles lying on the S_0 sheet are solely responsible for the system stability and oscillatory motion, because their response is exponential, $Ae^{\omega t}$, which can be

oscillatory and stable or unstable, accordingly as $\mathrm{Re}\,\omega \leq 0$ or $\mathrm{Re}\,\omega > 0$, respectively.

Calculation of Total Response

Finally, to complete the discussion of the solution for system response, the method of actually calculating the total response is necessary. A detailed description of the calculation of the inverse Laplace transform of the state vector transform, $\vec{X}(s)$, is given at the end of Example 1 in Chapter IV after the reader has become more familiar with the pole structure of systems of order 1/n. The calculation involves the evaluation of a contour integral in the s^1-plane.

Summary of Solution Process

1. Formulate the system of order 1/n (as illustrated in the examples).

2. Determine the optimal gain matrix $\tilde{K}$ through an algebraic Riccati equation solver, such as RICCATI in MATRIX$_X$, by using the equivalent first-order system, Eqs (37-40).

3. Solve the eigenvalue problem for the eigenvalues, λ, and eigenvectors, $\vec{\phi}$, in the $s^{1/n}$-plane.

4. Map the poles, λ, to the s^1-plane poles, ω.

5. Calculate the total response (as illustrated in Example 1).

IV. Example Problems

In this chapter the theory is demonstrated by numerical solution by finite element analysis of two examples of simple controlled structures. An iterative solution of the open loop equation of motion for the first mode eigenvectors and eigenvalues allows cross-checking the open loop eigenvalues and eigenvectors computed by matrix manipulation with MATRIX$_X$. The first example is a beam of viscoelastic material, pinned to allow only rotation at both ends. Both rotations are controlled. The second example is a long, thin aluminum rod, clamped at one end and damped by a viscoelastic pad at the other. Displacement is constrained to longitudinal motion and is controlled at the damped end.

These problems illustrate the method of applying the control theory to structures, as well as the technique of expanding the structure equation of motion into a differential system of order 1/n. The first problem has a lot of symmetry (damping, control, boundary conditions, geometry), while the second does not. The second shows how to incorporate both viscoelastic and elastic materials into a problem. The basic concept of finite element analysis does not change; viscoelastic materials are included in the element equation of motion and boundary conditions. The problems also show the technique of using MATRIX$_X$ to solve the Riccati and eigenvalue equations.

Example Problem 1: Simply-Supported Beam

Problem Statement: Given a simply-supported beam (pinned at both ends to allow only rotation) made of butyl B252 rubber as shown below, determine the open and closed poles to illustrate the effect of the linear feedback theory on system response, as described by rotational displacements θ_1 and θ_2 at nodes 1 and 2.

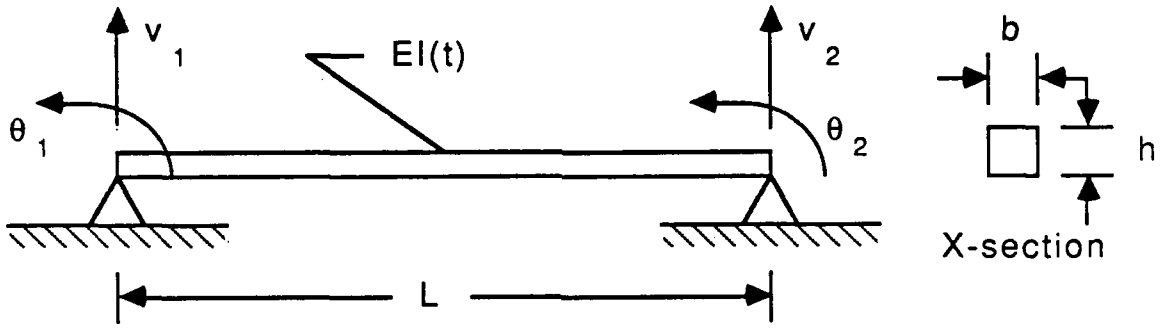

Figure 2. Example 1. Simply-supported Beam

Geometry:

L = 1.0 m

b = 0.1 m

h = 0.1 m

$I = bh^3/12 = 8.33E\text{-}6\ m^4$ (Moment of Inertia)

E = a time-dependent modulus to be described later in the Laplace domain

Boundary Conditions:

$v_1 = v_2 = 0$ (transverse linear displacements of nodes)

u_1 = control torque, determined by optimal control, u^*, on θ_1

u_2 = control torque, determined by optimal control, u^*, on θ_2

Stress-Strain Model

As Bagley (3:920) demonstrated, Butyl B252 rubber's tensile stress-strain relation, can be written in terms of a fractional derivative model of order α, which is determined by experiment involving sinusoidal excitation over a range of frequency $0 \leq \omega \leq 10^4$ cps:

$$\sigma(t) + bD_t^{\alpha}\sigma(t) = E_0\varepsilon(t) + E_1 D_t^{\alpha}\varepsilon(t) \tag{2}$$

where $\sigma(t)$ is the normal stress, $\varepsilon(t)$ is the normal strain, α = m/n (m, n are integers), and E_0 and E_1 are positive, constants. For this work b equals zero. In the time domain an operator, PE, acting on the strain, $\varepsilon(t)$, can be defined such that Eq (2) can be written as

$$\sigma(t) = PE(\varepsilon(t)) \tag{45}$$

In the Laplace domain, this operator can be described as a funtion, $\bar{E}(s)$, where the overbar denotes the Laplace transform domain, of the Laplace variable, s. This can easily be seen if one takes the Laplace transform of the general stress-strain model, which can be done since the model is linear. Assuming zero strain at t=0,

$$\bar{\sigma}(s) = E_0\,\bar{\varepsilon}(s) + \frac{E_1}{s^{1-\alpha}}\left[\, s\,\bar{\varepsilon}(s)\right]$$

$$\bar{\sigma}(s) = \left(E_0 + E_1 s^{\alpha}\right)\bar{\varepsilon}(s)$$

$$\bar{\sigma}(s) = \bar{E}(s)\,\bar{\varepsilon}(s) \tag{46}$$

The function $\bar{E}(s)$ is not a transform; it corresponds to an operator in the time domain and not to a function. This form of the time-

dependent modulus, i.e. $\bar{E}(s)$, is useful for applying the viscoelasticity correspondence principle (5:42). This principle states that in the Laplace domain the time-dependent modulus can be substituted for a presumed-elastic (constant) modulus, E, in an equation. Because the operator $PE(\varepsilon(t))$ can be expressed merely as an polynomial expression in s in the Laplace domain, it can be grouped as one term, as shown above. The correspondence principle says that E can be replaced by $\bar{E}(s)$ in the Laplace domain when viscoelastic loads are calculated using convolution which corresponds to multiplication in the Laplace domain. When viscoelastic materials are used in finite element models, the equation of motion (EOM) for an element is first derived assuming a constant modulus, E. The correspondence principle is then applied to the transform of the EOM. The resulting equation is solved for the response.

Based on Madigowski data, Bagley (3:920) has determined α and positive shear coefficients G_0 and G_1 in the shear stress-strain relationship for butyl rubber and several other materials:

$$\tau(t) = G_0\gamma(t) + G_1 D_t^{\alpha}\gamma(t) \tag{47}$$

where τ is shear stress and γ is the shear strain. To determine E_0 and E_1 one applies the basic relation between E_y, Young's modulus, and G, shear modulus, i.e. $E_y = 2(1+\nu)G$, where ν is the material's Poisson's ratio, and uses G_0 and G_1 to determine E_0 and E_1, respectively. For this work the rubber was assumed incompressible, so $\nu = 0.5$. Therefore,

Butyl B252 Rubber Values

$\rho = 0.92\ g/cm^3 = 920\ kg/m^3$

$\alpha = 0.5$

$G_0 = 760{,}000\ N/m^2$

$G_1 = 295{,}000\ Ns^{1/2}/m^2$

$E_0 = 2{,}280{,}000\ N/m^2$

$E_1 = 885{,}000\ Ns^{1/2}/m^2$

These figures are valid for $0 \leq$ frequency $\leq 10^4$ Hz.

Elastic Formulation of Equation of Motion

In finite element modelling the general equation of motion for a sturcture is formed by assembling the equations of motion of individual elements into one large system equation. The correspondence principle is applied to the element equation of motion for those elements containing the viscoelastic material. These modified equations are assembled into the system equation of motion, and the EOM is solved for the system response.

The general form of the equation of motion for an elastic finite element is

$$\tilde{m}\ddot{\vec{d}} + \tilde{k}\vec{d} = \vec{r} \qquad (48)$$

where

$\tilde{m}$ = element mass matrix (lumped or consistent)
$\vec{d}$ = element displacement vector
$\tilde{k}$ = element stiffness matrix
$\vec{r}$ = element applied nodal loads

Cook (7:87) gives the stiffness matrix for an elastic beam element as

$$\tilde{k} = \frac{EI}{L^3}\begin{bmatrix} 12 & 6L & -12 & 6L \\ 6L & 4L^2 & -6L & 2L^2 \\ -12 & -6L & 12 & 6L \\ 6L & 2L^2 & -6L & 4L^2 \end{bmatrix}$$

where E is the presumed-elastic modulus and the displacement vector is arranged by alternating translational and rotational displacements for each degree of freedom, i.e.

$$\vec{d} = \begin{pmatrix} v_1 \\ \theta_1 \\ v_2 \\ \theta_2 \end{pmatrix}$$

The applied element force vector, $\vec{r}$, brings in the control torques:

$$\vec{r} = \begin{pmatrix} 0 \\ u_1 \\ 0 \\ u_2 \end{pmatrix}$$

Since rotational displacements are of interest, Cook's consistent mass matrix must be used:

$$\tilde{M} = \frac{m}{420}\begin{bmatrix} 156 & 22L & 54 & -13L \\ 22L & 4L^2 & 13L & -3L^2 \\ 54 & 13L & 156 & -22L \\ -13L & -3L^2 & -22L & 4L^2 \end{bmatrix}$$

where

$m = \rho AL$ (A = cross-sectional area)

Since there is only one element in the structure, the assembled matrices, hence the equation of motion, are the element mass, stiffness, and force matrices. Applying the displacement boundary conditions reduces the system to two degrees of freedom:

$$\frac{\rho AL}{420}\begin{bmatrix} 4L^2 & -3L^2 \\ -3L^2 & 4L^2 \end{bmatrix}\begin{Bmatrix} \ddot{\theta}_1(t) \\ \ddot{\theta}_2(t) \end{Bmatrix} + \frac{EI}{L^3}\begin{bmatrix} 4L^2 & 2L^2 \\ 2L^2 & 4L^2 \end{bmatrix}\begin{Bmatrix} \theta_1(t) \\ \theta_2(t) \end{Bmatrix} = \begin{Bmatrix} u_1(t) \\ u_2(t) \end{Bmatrix}$$

or

$$\tilde{M}\begin{Bmatrix} \ddot{\theta}_1(t) \\ \ddot{\theta}_2(t) \end{Bmatrix} + E\tilde{K}'\begin{Bmatrix} \theta_1(t) \\ \theta_2(t) \end{Bmatrix} = \begin{Bmatrix} u_1(t) \\ u_2(t) \end{Bmatrix} \qquad (49)$$

where

$$\tilde{M} = \frac{\rho AL^3}{420}\begin{bmatrix} 4 & -3 \\ -3 & 4 \end{bmatrix}$$

$$\tilde{K}' = \frac{2I}{L}\begin{bmatrix} 2 & 1 \\ 1 & 2 \end{bmatrix}$$

Because E will be replaced by $\bar{E}(s)$, the stiffness matrix, $\tilde{K}$, has been identified as $E\tilde{K}'$.

Application of the Correspondence Principle

The Laplace transform, denoted by capital letters of functions, of the system is

$$\tilde{M}s^2\vec{\Theta}(s) + E\tilde{K}'\vec{\Theta}(s) = \vec{U}(s) \qquad (50)$$

where s is the Laplace variable and

$$\vec{\Theta}(s) = \begin{Bmatrix} \Theta_1(s) \\ \Theta_2(s) \end{Bmatrix}$$

$$\vec{U}(s) = \begin{Bmatrix} U_1(s) \\ U_2(s) \end{Bmatrix}$$

$\bar{E}(s)$ replaces E and gives the equation of motion in the Laplace domain:

$$\left[\tilde{M}s^2 + E_1 s^{1/2} \tilde{K'} + E_0 \tilde{K'} \right] \vec{\Theta}(s) = \vec{U}(s) \quad \text{(EOM)} \tag{51}$$

Open Loop Response

Recall from Chapter III that the Laplace variable s corresponds to the eigenvalue for a first-order system. Because the fractional derivative transforms have s to fractional powers, an eigenvalue λ is defined in the $s^{1/2}$-plane by $\lambda = s^{1/2}$, in order to have a polynomial with only integer powers. The eigenvector, $\vec{\phi}$, is given by the specific value of $\vec{\Theta}(s)$ for the eigenvalue λ. Then the open loop or homogeneous equation of motion is

$$\left[\tilde{M}\lambda^4 + E_1 \lambda \tilde{K'} + E_0 \tilde{K'} \right] \vec{\phi} = \vec{0} \tag{52}$$

which can be solved recursively for its first mode eigenvalue, λ_1, and eigenvector, $\vec{\phi}$, in the $s^{1/2}$-plane via an iterative routine (3:922-923):

$$\left[\lambda_1^{(n)} E_1 \tilde{K'} + E_0 \tilde{K'} \right]^{-1} \tilde{M} \, \vec{\phi}_1^{(n)} = - \frac{1}{\lambda_1^{4(n+1)}} \vec{\phi}_1^{(n+1)} \tag{53}$$

where (n) and $(n+1)$ are iteration steps. The routine steps are

1. Estimate $\lambda_1^{(1)}$, $\vec{\phi}_1^{(1)}$. Quality of guess only affects speed of convergence. For this thesis 1+i was simply used for $\lambda_1^{(1)}$. Undamped open loop first mode eigenvectors were used for $\vec{\phi}_1^{(1)}$.

2. Iterate on $\vec{\phi}_1$ holding $\lambda_1^{(n)}$ constant until the eigenvector converges, i.e. changes less than a tolerable difference.

3. Use new $\lambda_1^{(n+1)}$ and $\vec{\phi}_1^{(n+1)}$ as estimates for $\lambda_1^{(n)}$, $\vec{\phi}_1^{(n)}$.

4. Repeat steps 2 to 3 with until $\lambda_1^{(n)}$ converges.

Because it is a quartic equation, there are four values of $\lambda_1^{(n+1)}$ generated each iteration: $\lambda^{1/n} = A^{1/n}\{ \cos [(\Omega + 2\pi k)/n] + i \sin [(\Omega + 2\pi k)/n] \}$ where Ω is the argument of λ, A is the magnitude of λ, and k is an integer ranging from 0 to n-1. One value must be chosen for the iteration. Since each value corresponds to the possible solution on its branch or sector of the plane, the same solution must be pursued to gain convergence to the valid eigenvalue. Identification of branches is not difficult for open loop poles if one assumes that the pole argument does not vary greatly. Because fourth-roots are separated by $\pi/2$ radians, two can never lie in the same quadrant. Therefore, each branch can be identified by the signs of the real and imaginary parts. To maintain the same branch, always iterate with the root with the specified signs. This works well for open loop poles, but closed loop poles may move drastically from the open loop positions and into other quadrants. Improved algorithms for this situation have been studied currently by Captain Michele Devereaux (8).

Furthermore, because it is a quartic equation, there are four distinct eigenvalues for each eigenvector. The algorithm converges to only one at a time, so the iteration must be completed for each. Eigenvalues will always be real or occur in complex conjugate pairs because the coefficients are real. Moreover, there should be an open loop pole in each quadrant, because the viscoelastic model yields both exponential and power time response. The right two quadrants, because they map to the s^1-plane, give exponential response (stable or unstable); while the left two quadrants of the $s^{1/2}$-plane correspond to other planes in which poles give power response. Hence, one set of poles should be in the first and fourth quadrants; and one set should be in the second and third quadrant. There may be two negative real poles which correspond to lying on planes not shown in $s^{1/2}$-plane presentation. This procedure must be modified slightly for higher eigenvalues (3:922-923, 1:76-78).

Applying the problem values to the EOM matrices gives

$$\tilde{M} = 0.0219 \text{ kg-m}^2 \begin{bmatrix} 4 & -3 \\ -3 & 4 \end{bmatrix}$$

$$E_1\tilde{K} = 14.75 \text{ N-m} \begin{bmatrix} 2 & 1 \\ 1 & 2 \end{bmatrix}$$

$$E_0\tilde{K} = 38.0 \text{ N-m} \begin{bmatrix} 2 & 1 \\ 1 & 2 \end{bmatrix}$$

The mass matrix $\tilde{M}$ is multiplied by rad/sec^2 in the equation of motion. Thus, the final units are N-m, i.e. torque which is balanced in the equation of motion.

The controls analysis package (code) MATRIX$_X$ (14) was used to perform the iterative solution. MATRIX$_X$ has a feature called a command file (14:7-3 - 7-6) which allows a series of commands to be stored in an executable file. It is basically the equivalent of program. A MATRIX$_X$ command file entitled, 4th-order BEAM EigenValue Solver or 4BEAMEVS.EXC, was created to solve the recursive equation for the beam open loop eigenvalues of the first mode. The user supplies the assembled mass and stiffness matrices, as well as estimates for the first mode eigenvector and one of the eigenvalues. The program is interactive, and the user is asked to identify the desired root from the output and input it for iteration. The difference between past and present step values of the desired eigenvalue is displayed for both real and imaginary parts, and the user is queried about continuing the iteration on the branch. This could be automated, if desired. For this work the iteration was continued until the difference between past and present step values of the desired eigenvalue was less than 10^{-5} on both real and imaginary parts.

Because of the symmetry of the problem, especially the damping, the damping is expected to be proportional damping, i.e. the damping matrix $E_1\tilde{K}$ can be written as a linear combination of the mass and stiffness matrices (19:197). By inspection it is obvious that E_1K can be written in terms of the $E_0\tilde{K}$. In this case, the equations comprising the system can be decoupled, and the eigenvectors are the same as those for elastic system. The elastic first mode (19:213) is known to be

$$\vec{\phi}_1 = \begin{Bmatrix} 1 \\ -1 \end{Bmatrix} \tag{54}$$

and the first guess of the eigenvalue was $\lambda_1 = 1 + i$. Two conjugate pairs for the first mode result from the iteration:

$$\boxed{\lambda_1 = 2.9747 \pm 4.1150i \text{ and } -2.9747 \pm 0.8740i}$$

The poles with the positive real part correspond to vibrational motion, while the poles with the negative real part correspond to relaxational motion.

The iteration also gave the elastic first mode eigenvector, Eq (54), for all eigenvalues. This occurs because of the proportional damping.

These values can be checked because the first eigenvector is known. By premultiplying by the transpose of the jth eigenvector Eq (52) reduces to a fourth-order scalar polynomial in λj:

$$\vec{\phi}_j^T \left[\lambda_j^4 \tilde{M} + \lambda_j E_1 \tilde{K} + E_0 \tilde{K} \right] \vec{\phi}_j = 0$$

By using a root finding routine, such as the ROOTS command (14:4-16) in MATRIX$_X$, the eigenvalues are found to be the same. The elastic second mode is also known:

$$\vec{\phi}_2 = \begin{Bmatrix} 1 \\ 1 \end{Bmatrix} \tag{55}$$

and the eigenvalues can be found by the same method:

$$\boxed{\lambda_2 = 7.1139 \pm 11.0272i \text{ and } -11.6288, -2.5989}$$

The poles with the positive real part correspond to vibrational motion, while the poles with the negative real part correspond to relaxational motion.

1/2-Order System Formulation

The general problem can be posed in a fractional state-space by a 1/2th-order system (3:921-922). A fractional state-space is defined as a state-space in which fractional as well as integer derivatives of variables are included in the state vector, e.g.

$$\underline{\vec{\theta}}(t) = \begin{Bmatrix} D_t^{3/2}\vec{\theta}(t) \\ D_t^{1}\vec{\theta}(t) \\ D_t^{1/2}\vec{\theta}(t) \\ \vec{\theta}(t) \end{Bmatrix}$$

or

$$\underline{\vec{\Theta}}(s) = \begin{Bmatrix} s^{3/2}\vec{\Theta}(s) \\ s^{1}\vec{\Theta}(s) \\ s^{1/2}\vec{\Theta}(s) \\ \vec{\Theta}(s) \end{Bmatrix}$$

whe4m states:

$$s^{1/2}\begin{bmatrix} \tilde{0} & \tilde{0} & \tilde{0} & \tilde{M} \\ \tilde{0} & \tilde{0} & \tilde{M} & \tilde{0} \\ \tilde{0} & \tilde{M} & \tilde{0} & \tilde{0} \\ \tilde{M} & \tilde{0} & \tilde{0} & E_1\tilde{K} \end{bmatrix}\begin{Bmatrix} s^{3/2}\vec{\Theta}(s) \\ s^{1}\vec{\Theta}(s) \\ s^{1/2}\vec{\Theta}(s) \\ \vec{\Theta}(s) \end{Bmatrix} + \begin{bmatrix} \tilde{0} & \tilde{0} & -\tilde{M} & \tilde{0} \\ \tilde{0} & -\tilde{M} & \tilde{0} & \tilde{0} \\ -\tilde{M} & \tilde{0} & \tilde{0} & \tilde{0} \\ \tilde{0} & \tilde{0} & \tilde{0} & E_0\tilde{K} \end{bmatrix}\begin{Bmatrix} s^{3/2}\vec{\Theta}(s) \\ s^{1}\vec{\Theta}(s) \\ s^{1/2}\vec{\Theta}(s) \\ \vec{\Theta}(s) \end{Bmatrix}$$

$$= \begin{bmatrix} \tilde{0} \\ \tilde{0} \\ \tilde{0} \\ \tilde{I} \end{bmatrix} \vec{U}(s) \qquad (56)$$

where $\tilde{0} = \begin{bmatrix} 0 & 0 \\ 0 & 0 \end{bmatrix}$ and $\tilde{I} = \begin{bmatrix} 1 & 0 \\ 0 & 1 \end{bmatrix}$. This is rearranged to

$$s^{1/2}\vec{\Theta}(s) = \tilde{A}\,\vec{\Theta}(s) + \tilde{B}\,\vec{U}(s) \qquad (57)$$

where

$$\tilde{A} = -\begin{bmatrix} \tilde{0} & \tilde{0} & \tilde{0} & \tilde{M} \\ \tilde{0} & \tilde{0} & \tilde{M} & \tilde{0} \\ \tilde{0} & \tilde{M} & \tilde{0} & \tilde{0} \\ \tilde{M} & \tilde{0} & \tilde{0} & E_1\tilde{K} \end{bmatrix}^{-1} \begin{bmatrix} \tilde{0} & \tilde{0} & -\tilde{M} & \tilde{0} \\ \tilde{0} & -\tilde{M} & \tilde{0} & \tilde{0} \\ -\tilde{M} & \tilde{0} & \tilde{0} & \tilde{0} \\ \tilde{0} & \tilde{0} & \tilde{0} & E_0\tilde{K} \end{bmatrix}$$

$$\tilde{B} = \begin{bmatrix} \tilde{0} & \tilde{0} & \tilde{0} & \tilde{M} \\ \tilde{0} & \tilde{0} & \tilde{M} & \tilde{0} \\ \tilde{0} & \tilde{M} & \tilde{0} & \tilde{0} \\ \tilde{M} & \tilde{0} & \tilde{0} & E_1\tilde{K} \end{bmatrix}^{-1} \begin{bmatrix} \tilde{0} \\ \tilde{0} \\ \tilde{0} \\ \tilde{I} \end{bmatrix}$$

To complete the system, it is assumed that all states are outputs and that there is no feedforward to the output, i.e.

$$\vec{Y}(s) = \tilde{C}\vec{\Theta}(s) + \tilde{D}\,\vec{U}(s)$$

where

$\tilde{C}$ = 4m x 4m identity matrix
$\tilde{D}$ = m x q null (zero) matrix (q = number of control inputs)

For the specific problem m=2 and q = 2, so the system has eight states and two control inputs.

Open Loop Poles via MATRIX$_X$

If the control vector is set to zero, i.e. $\vec{0}$, in the 1/nth-order system, Eq (57) reduces to an eigenvalue problem. However, there will be m sets of eigenvalues, where m is the number of degrees of freedom again. Eigenvalues and eigenvectors of the A matrix were determined by the EIG command of MATRIX$_X$ (14:4-23). These corresponded to the first two modes. The first mode eigenvalues and eigenvectors determined by the recursive solution of the open loop equation of motion, Eq (52), match those determined by MATRIX$_X$.

Closed Loop Poles via MATRIX$_X$

Solution for closed loop poles and eigenvectors is quite easy on MATRIX$_X$. First, the system must be posed for the Riccati Equation solver in the appropriate $\tilde{A}^n - \tilde{A}^{n-1}\tilde{B}$ form, as indicated in Chapter III:

$$\dot{\vec{\theta}}(t) = \tilde{A}^n \vec{\theta}(t) + \tilde{A}^{n-1}\tilde{B}\,\vec{u}(t)$$

Therefore, for this example

$$\dot{\vec{\theta}}(t) = \tilde{A}^2 \vec{\theta}(t) + \tilde{A}\tilde{B}\,\vec{u}(t) \qquad (58)$$

The MATRIX$_X$ Riccati solving command, called RICCATI (14:14-19), was used to determine the optimal gain matrix, $\tilde{P}$, such that

$$\vec{u}^{*}(t) = -\tilde{R}^{-1}\tilde{B}^{T}\tilde{A}^{n-1\,T}\tilde{P}\,\vec{\theta}(t) \qquad (59)$$

However, the routine also output the overall gain matrix, $\widetilde{KC}$, where

$$\widetilde{KC} = \tilde{R}^{-1}\tilde{B}^{T}\tilde{A}^{n-1\,T}\tilde{P}$$

and this matrix was used in the calculation of closed loop poles. RICCATI($\tilde{S}$,$\widetilde{RQ}$,NS) requires three inputs: a system matrix ($\tilde{S}$), a performance index weighting matrix ($\widetilde{RQ}$), and the number of states (NS) in the state vector. These are

$$\tilde{S} = \begin{bmatrix} \tilde{A}^{n} & \tilde{A}^{n-1}\tilde{B} \\ \tilde{C} & \tilde{D} \end{bmatrix}$$

$$\widetilde{RQ} = \begin{bmatrix} \tilde{Q} & \widetilde{N_R} \\ \widetilde{N_Q} & \tilde{R} \end{bmatrix}$$

$NS = 4m$

where

$\widetilde{N_Q}$ = 4m x 4m null matrix (same dimensions as $\tilde{Q}$)
$\widetilde{N_R}$ = 4m x q null matrix (same dimensions as $\tilde{R}$)
m= 2 for this problem
q = 2 for this problem

For this problem m= 2 and q = 2. The closed loop system, Eq (58), becomes an eigenvalue problem once the gain matrix for the optimal steady-state linear feedback is known. The Laplace transform of Eq (58) is

$$s^{1/2}\vec{\Theta}(s) = \left(\tilde{A} - \tilde{B}\tilde{R}^{-1}\tilde{B}^{T}\tilde{A}^{T}\tilde{P}\right)\vec{\Theta}(s) \qquad (59)$$

For this specific problem the inputs to RICCATI are

$$\tilde{S} = \begin{bmatrix} \tilde{A}^2 & \tilde{A}\tilde{B} \\ \tilde{C} & \tilde{D} \end{bmatrix}$$

$$\widetilde{RQ} = \begin{bmatrix} \tilde{0} & \tilde{0} & \tilde{0} & \tilde{0} & \tilde{0} \\ \tilde{0} & \tilde{I} & \tilde{0} & \tilde{0} & \tilde{0} \\ \tilde{0} & \tilde{0} & \tilde{0} & \tilde{0} & \tilde{0} \\ \tilde{0} & \tilde{0} & \tilde{0} & \tilde{I} & \tilde{0} \\ \tilde{0} & \tilde{0} & \tilde{0} & \tilde{0} & \tilde{I} \end{bmatrix}$$

NS = 8

MATRIX$_X$ then gives $\tilde{P}$ and $\widetilde{KC}$:

P = 1000 *

0.0000	0.0000	-0.0001	0.0001	0.0002	-0.0001	0.0025	-0.0008
0.0000	0.0000	-0.0001	0.0001	0.0002	-0.0001	0.0025	-0.0008
0.0000	0.0000	0.0001	-0.0001	-0.0001	0.0002	-0.0008	0.0025
-0.0001	0.0001	0.0005	-0.0003	-0.0025	0.0008	0.0000	0.0000
0.0001	-0.0001	-0.0003	0.0005	0.0008	-0.0025	0.0000	0.0000
0.0002	-0.0001	-0.0025	0.0008	0.0186	0.0021	0.0409	-0.0091
-0.0001	0.0002	0.0008	-0.0025	0.0021	0.0186	-0.0091	-0.0409
0.0025	-0.0008	0.0000	0.0000	-0.0409	-0.0091	2.2763	1.7681
-0.0008	0.0025	0.0000	0.0000	-0.0091	-0.0409	1.7681	2.2763

$\widetilde{KC}$ =

-0.6380	0.1986	5.6916	0.6239	-48.2600	-26.8662	0.0088	-0.0044
0.1986	-0.6380	0.6239	5.6916	-26.8662	-48.2600	-0.0044	0.0088

MATRIX$_X$'s EIG command (14:4-23) solves the closed loop eigenvalue problem for the closed loop poles and eigenvectors of both modes. The poles are given in a jumbled order:

7.2744 +11.2328i
7.2744 -11.2328i

-0.2318 + 3.0553i
2.9596 + 4.2008i
2.7549 + 4.6337i
-0.2318 - 3.0553i
2.9596 - 4.2008i
2.7549 - 4.6337i

The command EIG does not identify which closed poles correspond to which open loop poles. In general, if the open loop poles are known for each mode, the closed loop poles for each mode can be identified. Starting from the open loop system, feedback gain is increased from zero to full value in small enough steps to see the poles move from open loop to closed loop positions. The tracks map each open loop pole to its closed loop position. In controls analysis this plot is called a root-locus. The eigenvalues for each mode of the specific problem are

$$\lambda_1 = 2.9596 \pm 4.2008i \text{ and } -0.2318 \pm 3.0553i$$
$$\lambda_2 = 7.2744 \pm 11.2328i \text{ and } 2.7549 \pm 4.6337i$$

The eigenvectors, as determined by the EIG command, remain the same as the open loop eigen vectors, which are the elastic eigenvectors Eqs (54) and (55). This makes identification of the poles easy.

The closed loop poles can be determined by creating a scalar equation using the known eigenvectors, as in the open loop case. The control vector is replaced in the system, Eq (58), by the optimal control vector, which is $\widetilde{KC}\vec{\phi}$. The vector is brought to the left-hand side of the equation. The scalar equation of motion is given by the bottom m rows, where m is the number of degrees of freedom,

of the system equation and now has non-zero coefficients for λ^3 and λ^2 and becomes

$$\vec{\phi}_j^T \left[\lambda_j^4 \widetilde{M} + \lambda_j^3 \widetilde{KC}_{1m} + \lambda_j^2 \widetilde{KC}_{2m} + \lambda_j \left(E_1 \widetilde{K} + \widetilde{KC}_{3m} \right) + \left(E_0 \widetilde{K} + \widetilde{KC}_{4m} \right) \right] \vec{\phi}_j = 0$$

where $\widetilde{KC}_{qm}$ is the qth set of m columns of $\widetilde{KC}$. The first and second mode eigenvalues are found to be the same as the quoted above. The Bagley and Torvik algorithm can be modified to solve this new eigenvalue problem. Unless the eigenvectors are known, the only other means of determining which eigenvalues belong to which modes is the iterative method of increasing gain.

Measures of Change in Stability

A quick check for increased stability can be done by comparing pole positions: are closed loop poles further left (i.e. real part) than open loop poles, and do closed loop poles have a larger ratio of imaginary to real components?

In the s^1-plane the real component equals $-\zeta\omega_n$, where ζ is the damping ratio and ω_n is the natural frequency. The amplitude of the response is driven by $e^{-\zeta\omega_n t}$. Consequently, pole movement further left on the real axis results in a more negative exponent; and, the system amplitude dies faster. A measure of this motion is given by the difference between open and closed loop real components. Mapping poles between the $s^{1/2}$- and s^1-planes will effect the magnitude of the value but will not change the sign which identifies the direction of motion (plus means left and negative right).

The imaginary component of the pole in the s^1-plane is ω_d, the damped frequency. Therefore, the ratio of imaginary to real components gives a measure of both the damping ratio and the damped frequency with respect to the natural frequency. Moreover, the cosine of angle between the negative real axis and a line drawn between the pole and the origin is the damping ratio, ζ. The larger the angle the smaller is the damping ratio, which means less damping. The ratio of real to imaginary parts, thus, is also a measure of ζ. Since stable response poles lie in the two $s^{1/2}$-plane sectors $\pi/4 \leq \theta \leq \pi/2$ and $-\pi/2 \leq \theta \leq -\pi/4$, a higher ratio puts a pole closer to the imaginary axis (larger tan θ; hence, larger θ) than another. Therefore, it maps closer to the real axis in the s^1-plane and has a lower damped frequency and higher damping ratio, ζ.

Because the poles in the left half $s^{1/2}$-plane do not lie on the s^1-plane and, thus, do not contribute to typical stability measures, their movement with respect to stability is less clear. These poles cause negative-power time response which decays slower than an exponential response. If they move right or increase their imaginary-to-real ratio, they move toward the s^1-plane. If they move onto the left half of the s^1-plane, their response is more stable than before, because the poles now cause decaying exponential response. Therefore, motion right and increasing ratios of poles in the left half $s^{1/2}$-plane would seem to indicate increased system stability. Under these rules these two measures, difference between real components and imaginary-to-real ratio, give measures of the change in stability of the system.

Comparison of Open and Closed Loop Poles

The open loop eigenvalues of the first and second modes are shown in Figure 3.

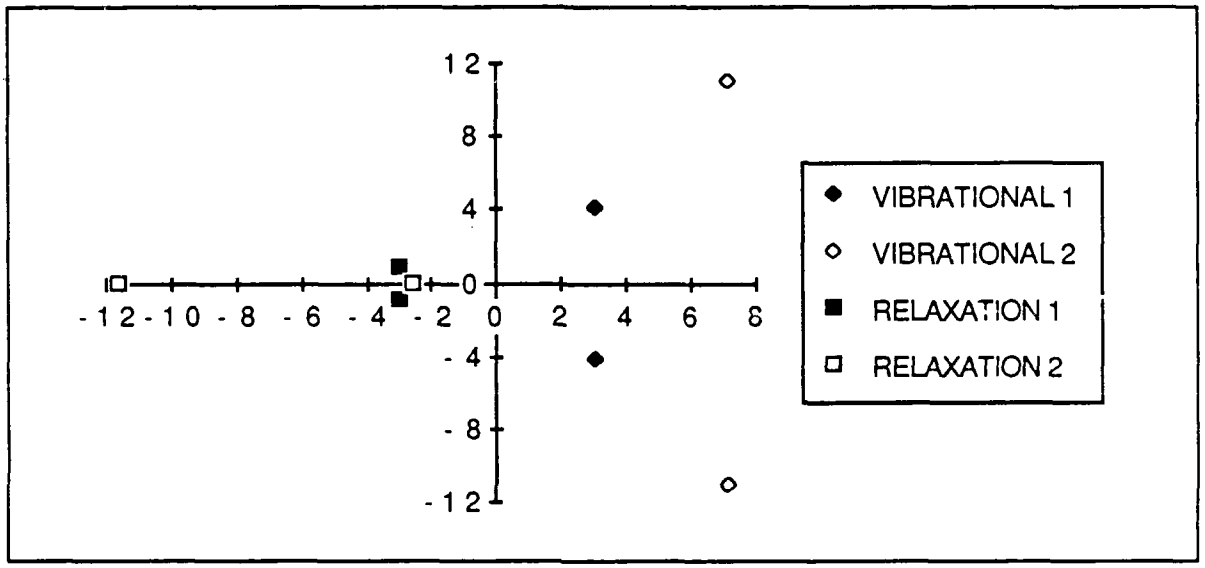

Figure 3. Example 1 Open Loop Poles for Both Vibrational and Relaxation Modes 1 and 2.

and the closed loop eigenvalues are shown graphically in Figure 4.

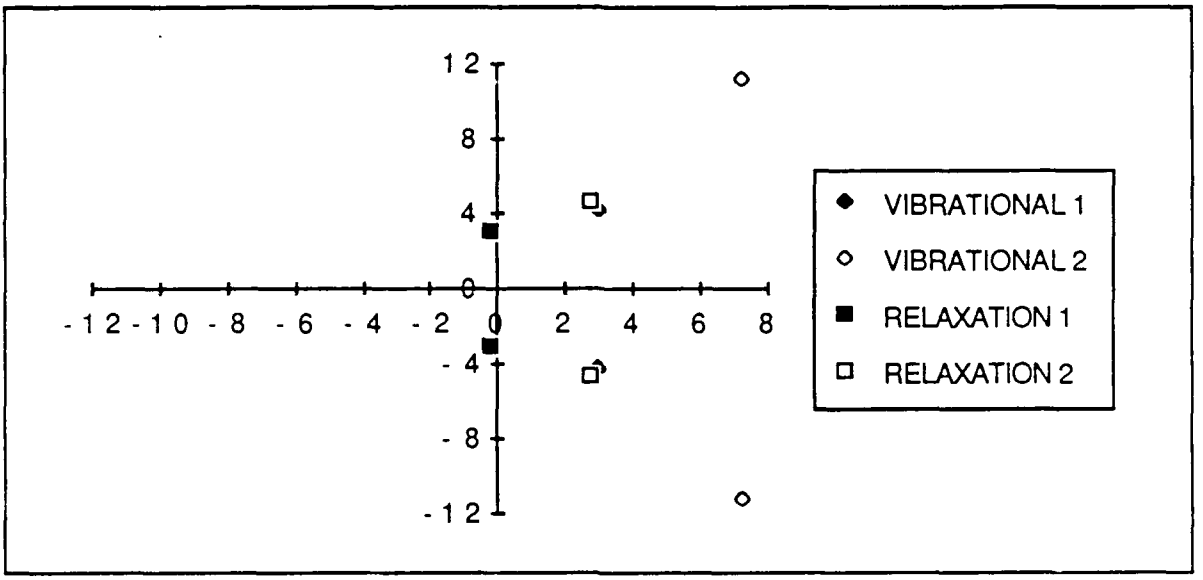

Figure 4. Example 1 Closed Loop Poles for Both Vibrational and Relaxation Modes 1 and 2.

Real components of the open and closed loop eigenvalues, Re(O) and Re(C) respectively, the difference between the open and closed loop real parts, denoted by Re(O)-Re(C), and ratios of the imaginary to real parts, denoted by I/R, for the first two modes are tabulated in Table I. A negative number in the Re(O)-Re(C) column indicates the poles have moved right.

Table I. Stability Measures for Example 1

Mode	Re(O)	Re(C)	Re(O)-Re(C)	Open I/R	Closed I/R
1	2.9747	2.9596	0.0151	1.3833	1.4194
	-2.9747	-0.2318	-2.7429	0.2938	13.1808
2	7.1139	7.2744	-0.1605	1.5501	1.5442
	-11.6288	2.7549	-14.3837	0.0	1.6820
	-2.5989	2.7549	-5.3538	0.0	1.6820

The data from this table shows that optimal control does not necessarily mean most stable for all poles. The first two eigenvalues, which represent the exponential response of the s^1-plane, of the first mode increased in stability, as indicated by the motion left of the real part (positive difference Re(O)-Re(C)) and by the increase of the imaginary-to-real ratio, I/R. However, the positive-real-part eigenvalues of the second mode destabilized slightly, as shown by the motion right of the real part (negative difference Re(O)-Re(C)) and a decrease in the I/R ratio. The second mode poles which have negative real parts moved right far enough to enter the region corresponding to the left half s^1-plane. Therefore, these poles, which

formerly gave non-oscillatory relaxation response, now give a vibrational response! Furthermore, the poles lie nearly on top of the positive-real-part poles of the first mode. Because of the first and second mode eigenvectors, Eqs (54) and (55), there is constructive interference at node 1 and destructive interference at node 2. Finally, the negative-real-part eigenvalues of the first mode also destabilized by moving right but has increased its damping ratio and lowered its damped frequency, as indicated by the increased I/R ratio.

Most of the closed loop poles are not very far from the open loop poles. It would appear that these values are already fairly optimal under the current evenly-weighted performance index. The problem appears to be heavily, perhaps overly, damped, and the

destabilization of the one pole may represent a desire for the system to be less damped. By destabilizing the pole the system would appear more flexible.

The system is stable with the optimal feedback, which produces significant changes in the response. However, this system is not very indicative of large, flexible space structures because of the geometry, i.e. this system is heavy weight. Furthermore, there is so much damping material that the system is probably overdamped and does not need much feedback, if any. Therefore, a problem more representative of the structures of interest is needed.

Modified Beam Geometry to Represent a Flexible Space Structure

Such a problem can be achieved by a modification of the geometry to represent a more slender beam. Therefore, let b = h = 0.01m . This divides $\tilde{M}$ by 100 and divides $\tilde{K}'$ by 10^4. The open loop eigenvalues are

$$\lambda_{1,OL} = 0.8936 \pm 1.0333i$$
$$-0.8936 \pm 0.7276i$$

and

$$\lambda_{2,OL} = 1.9573 \pm 2.5320i$$
$$-1.9573 \pm 1.1183i$$

and are shown graphically in Figure 5.

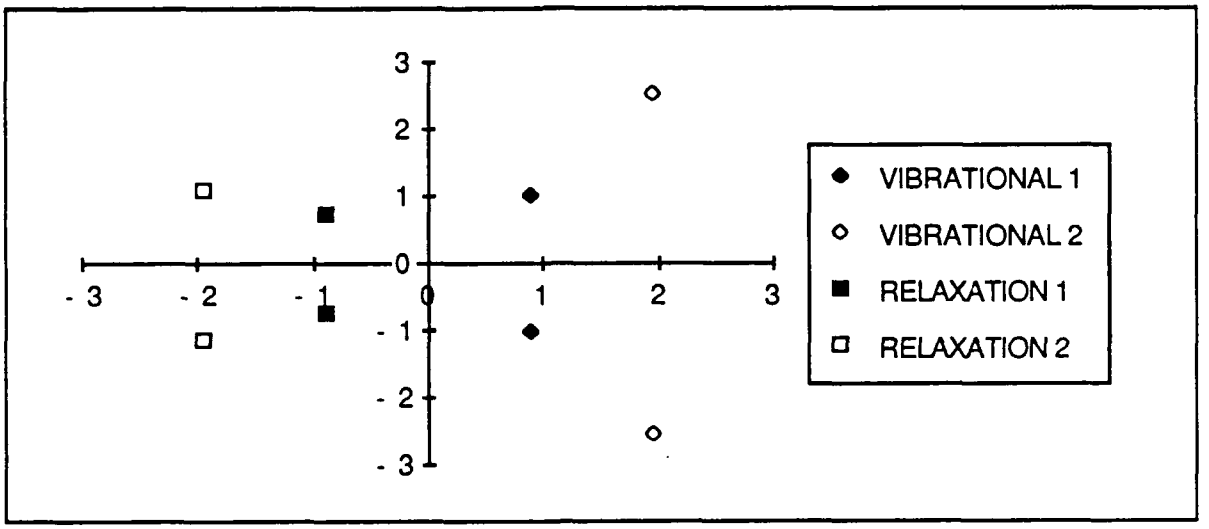

Figure 5. Modified Example 1 Open Loop Poles for Both Vibrational and Relaxation Modes 1 and 2.

By following the same procedures outlined earlier, the gain matrix $\widetilde{KC}$ is determined to be

$$\widetilde{KC} =$$

$$\begin{bmatrix} -0.0007 & 0.0001 & 1.0009 & -0.0007 & -0.0036 & -0.0014 & 0.9924 & -0.0038 \\ 0.0001 & -0.0007 & -0.0007 & 1.0009 & -0.0014 & -0.0036 & -0.0038 & 0.9924 \end{bmatrix}$$

The closed loop eigenvalues are

$$\lambda_{1,CL} = 0.2583 \pm 25.5363i$$
$$0.0000 \pm 1.0000i$$

and

$$\lambda_{2,CL} = 1.3870 \pm 67.5522i$$
$$0.0000 \pm 1.0000i$$

and are shown graphically in Figure 6.

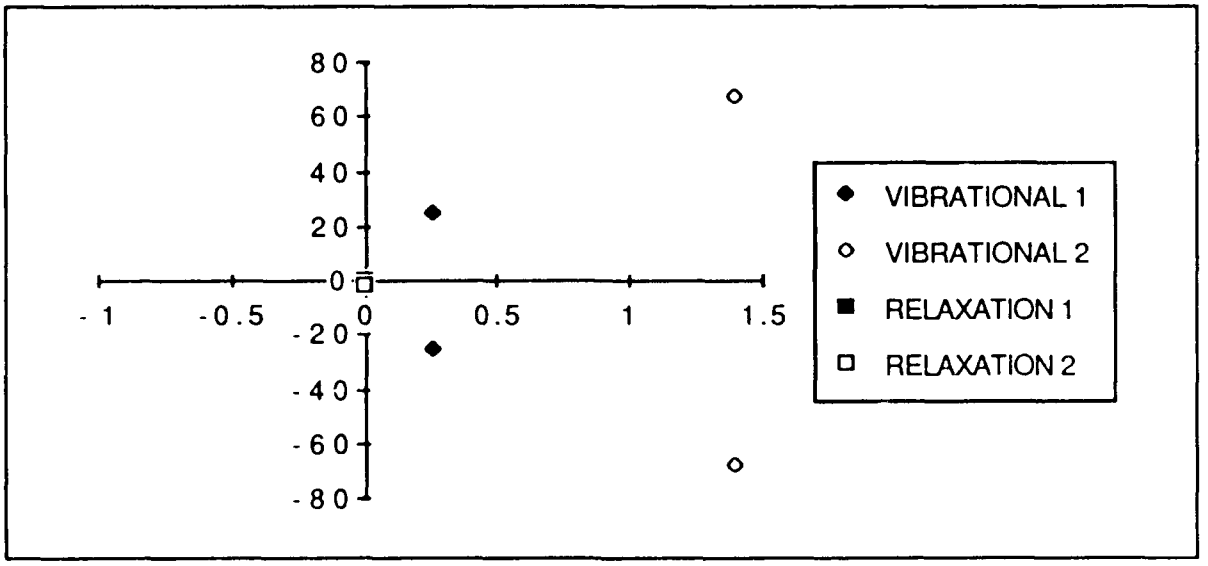

Figure 6. Modified Example 1 Closed Loop Poles for Both Vibrational and Relaxation Modes 1 and 2.

The stability measures for the poles are shown in Table II.

Table II. Stability Measures for Modified Example 1

Mode	Re(O)	Re(C)	Re(O)-Re(C)	Open I/R	Closed I/R
1	0.8936	0.2583	0.6353	1.1563	98.8630
	-0.8936	0.0	-2.7429	0.8142	∞
2	1.9573	1.3870	0.5703	1.2936	48.7038
	-1.9573	0.0	-1.9573	0.5713	∞

The data in Table II shows stability increases with the optimal feedback control for the positive-real-part poles of both first and second modes. These poles have moved left (positive Re(O)-Re(C))

and have dramatically increased their imaginary-to-real (I/R) ratios. The latter indicates a significant increase in damping ratio, ζ, as will as a significant decrease in the damped frequency. Once again, the negative-real-part poles moved right (negative Re(O)-Re(C)) as well as increased their I/R ratios. In fact, these poles achieved the maximum value of the I/R ratio. They have moved to the imaginary axis and will map to the negative real axis in the s^1-plane. Therefore, these poles, which previously gave relaxation (power-law) response, now give purely monotonically decaying exponential response.

The positive-real-part poles produce the characteristic damping and frequency parameters for the oscillatory motion. The eigenvalues in the $s^{1/2}$-plane and s^1-plane, denoted by EV $s^{1/2}$ and EV s^1 respectively, and oscillatory motion parameters, which are damping ratio (ζ), natural frequency (ω_n), and damped frequency (ω_d), are shown in Table III.

Table III. Example 1 Oscillatory Motion Parameters

EV $s^{1/2}$	EV s^1	ζ	ω_n	ω_d
Open Loop				
0.8936 ± 1.0333i	-0.2692 ± 1.8467i	0.1442	1.8669	1.8467
1.9573 ± 2.5320i	-2.5800 ± 9.9118i	0.2519	10.2422	9.9118
Closed Loop				
0.2583 ± 25.5363i	-652.04 ± 13.192i	0.9998	652.17	13.192
1.3870 ± 67.5522i	-4561.4 ± 187.39i	0.9992	4565.1	187.39

The data shows a tremendous improvement in system response. The damping ratio, ζ, becomes nearly equal to one, i.e. critical damping, which causes the system response to approach equilibrium faster than any other damped response. The resonant frequencies have been driven up to much higher frequencies. Therefore, the oscillatory motion dies much faster, because $e^{-\zeta\omega_n t}$ governs the decay of the envelope of the motion amplitude. Also, the ability to excite the structure, by simple handling or operation, has been reduced, e.g. it would not be excited by merely walking on it. Furthermore, the resonant mode separation has been increased from 8.375 rad/sec to 3913 rad/sec. This effectively isolates one mode from another, and controllers can neutralize one mode with less excitation on another. These results show conclusively that the optimal linear feedback control utilizing fractional state-space can successfully and significantly increase system stability.

Contribution of Each Derivative to Pole Structure

Structures have been controlled by position, velocity, and acceleration feedback in the past. What benefit lies in also feeding back fractional states? Insight to the answer can be gained by feeding back only one derivative at a time.

For example, feeding back only velocity (using the optimal gains determined for the fractional state model) yields poles further left than those from feeding back the entire state matrix: $0.0007 \pm 25.5571i$ and $0.0022 \pm 67.5737i$ which map to $-653.16 \pm 0.0358i$ and $-4566.2 \pm 0.2973i$. Although these have a

better damping ratio, they do not minimize the performance index. More highly damped is not necessarily optimal. However, this does show that the velocity is a major player in shifting the poles left.

If the 3/2-derivative is fed back alone, the $s^{1/2}$-plane poles are $1.0466 \pm 1.0243i$ and $2.9034 \pm 2.3290i$. The poles have moved right and have even become unstable! Therefore, the 3/2-derivative would counteract some of the strong stabilizing influence of the first derivative, so that the performance index is minimized further than by using velocity alone. This last statement derives from the fact that the optimization of the gain did not zero the gain for the 3/2-derivative. If the poles of the velocity-only feedback minimized the performance index, then this zeroing would occur.

If both 3/2-derivative and first derivative are fed back, then the poles become nearly the final optimal values: $0.2590 \pm 25.5558i$ and $1.3892 \pm 67.5595i$ where $0.2583 \pm 25.5363i$ and $1.3870 \pm 67.5522i$ are the optimal poles in the $s^{1/2}$-plane. Hence, these derivatives are responsible for the majority of the movement of the poles.

If the other derivatives are fed back individually, a pattern emerges. The odd half-derivatives (1/2, 3/2, etc) move the poles right, and the even half-derivatives (0, 1, etc) move the poles left. Furthermore, the higher the derivative the greater is its effect in each category. So, a 3/2-derivative moves the poles more than a 1/2-derivative. The gains of each are traded off to minimize the performance index with the lower derivatives acting as fine tuners.

Because the higher derivatives result in higher order polynomials in the feedback transfer function, they can contribute more poles to move the root-locus left in the s^1-plane. Take, for example, a general negative feedback system with plant transfer function G(s) and feedback transfer function H(s) in the $s^{1/2}$-plane. The characteristic equation is $1 + G(s)H(s) = 0$. If h(t) is a 1/2-derivative, then its transform in the $s^{1/2}$-plane is $H(s) = As$, where A is a constant. H(s) can generate only one pole (root of the characteristic equation) for the system, because H(s) increases the orderof the characteristic equation by only one. However, if h(t) is a 3/2-derivative, then H(s) equals As^3 and generates three poles because it raises the order by three. Location of the poles moves the root-locus left or right, but more poles will cause more effect than less. Therefore, the higher derivatives have more of an effect on the pole structure.

Calculation of Total Response

Finally, to complete the discussion of system response and stability, the method of actually calculating the total response is necessary. This will hopefully clarify how the poles which have been neglected so far (i.e. those not on the s^1-plane) are accounted for in the total response.

Bagley, in his dissertation (1), and Bagley and Torvik (2:747-748) describe the calculation of a system response to impulsive loading. Fundamentally, the inverse Laplace transform of the displacement vector, $L^{-1}[\vec{X}(s)]$, where s is the Laplace variable and

the capital X indicates the Laplace transform of the state vector, must be calculated. By definition, the inverse transform is a contour integration in the s^1-plane, as shown in Figure 3. Segments 3, 4, and 5 are required because of the branch cut on the negative real axis.

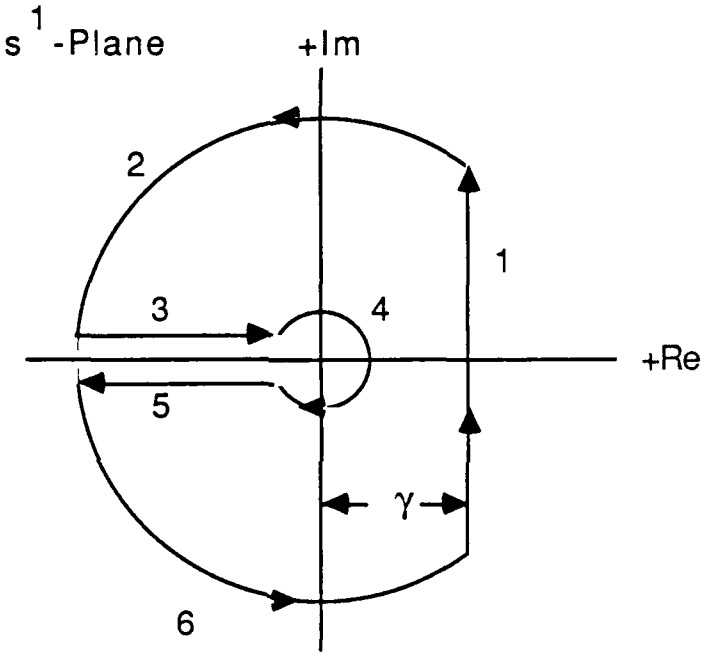

Figure 7. Integration Contour to Calculate Response

The inverse Laplace transform of $\vec{X}(s)$ is defined as

$$L^{-1}[\vec{X}(s)] = \frac{1}{2\pi i}\int_{\gamma-i\infty}^{\gamma+i\infty} e^{st}\,\vec{X}(s)\,ds.$$

The segment of the contour which produces the inverse transform $L^{-1}[\vec{X}(s)]$ is segment 1. The transform $\vec{X}(s)$ can be written as a

summation of the 4m eigenvalues and eigenvectors, where m is the number of degrees of freedom.

$$\vec{X}(s) = \sum_{n=1}^{4m} \frac{\vec{\phi}_n^T \vec{F}(s)\ (1+bs^{\alpha})}{m_n\ (s^{1/\alpha}-\lambda_n)} \vec{\phi}_n$$

where

$\vec{\phi}_n$ = nth eigenvector of the non-expanded equation of motion

$\vec{F}(s)$ = transform of the non-expanded applied force vector

$\underline{\vec{\phi}}_n$ = nth eigenvector of the expanded equation of motion

$\underline{\tilde{M}}$ = the expanded mass matrix which is the coefficient matrix associated with the $s^{1/2}$ term in Eq (56), an early form of the expanded system, Eq (57)

$m_n = \underline{\vec{\phi}}_n^T \underline{\tilde{M}}\ \underline{\vec{\phi}}_n$ = a modal constant

Since both open and closed systems have the form of an unforced (homogeneous) system, the response is determined by examining the impulse response. This also assumes that all initial conditions are zero. Therefore, $\vec{F}(s) = \vec{1}$, vector of ones, because the impulse is applied to all nodes. Also recall that b=0 for this problem. Another important point is that there are eight eigenvalues and eigenvectors from the expanded equation of motion but only two modes. The eigenvectors of the expanded equation of motion are distinct, but the mode shapes of physical deflection are not. If the eigenvectors had complex elements, we would have seen complex conjugate pairs of

eigenvectors. This is shown in Bagley's and Torvik's example in their paper (2:746).

By including the transform in the contour integration and using the residue theorem from complex calculus, the transform can be written in terms of a sum of the integrals for the other five segments and a sum of the residues:

$$\frac{1}{2\pi i}\int_{\gamma-i\infty}^{\gamma+i\infty} e^{st}\,\vec{X}(s)\,ds = \frac{1}{2\pi i}\sum_{k=2}^{6}\int_{k} e^{st}\,\vec{X}(s)\,ds + \sum_{j}\vec{b}_j$$

where $\vec{b}_j$ are the residues of the poles enclosed by the contour. The residues can be shown to produce the exponential response related to the s^1-plane poles. Bagley (4:141-143) has shown that the integrals for segments 2, 4, and 6 are zero, when radii of 2 and 6 increase toward infinity and the radius of 4 approaches zero. He has also shown that over long time the integrals for segments 3 and 5 asymptotically approach $t^{-\eta}$ for t large, where $\eta > 1$. It is in these integrals that the effect of the poles not on the s^1-plane becomes included in the overall response. Only here are they included in the response calculation because of the form of $\vec{X}(s)$. As has been noted earlier, this portion of the response correlates to the power-law stress relaxation observed by Nutting (11) in deformed materials.

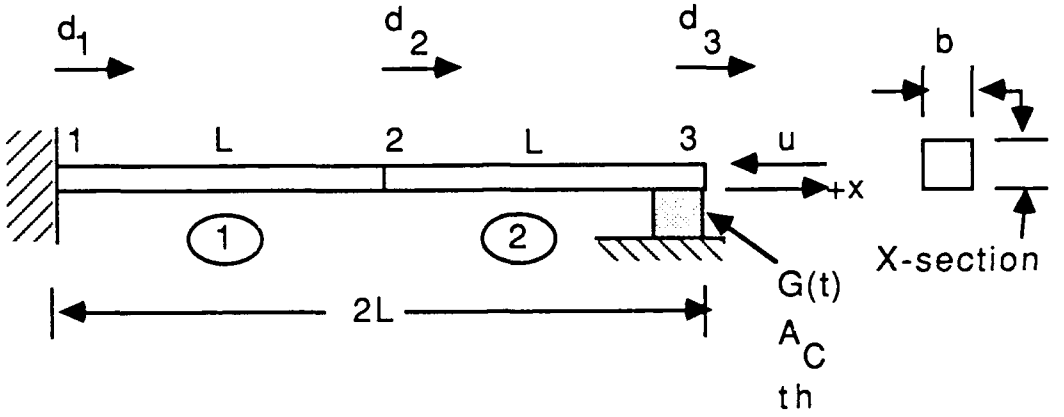

Figure 8. Example 2. Fixed-Shear Rod Diagram

Geometry and Properties

L= 1 m

b = h = 0.01m

ρ = 2796 kg/m^3

E = 6.894 x 10^{10} N/m^2

A_c = 0.0001 m (area of contact between shear pad and rod)

th = 0.01 m

G(s) = $G_0 + G_1 s^{1/2}$ (shear modulus defined in the Laplace domain)

G_0 = 7.6 x 10^5 N/m^2

G_1 = 2.95 x 10^5 Ns$^{1/2}$/m^2

Boundary Conditions and Applied Forces

d_1 = 0

τ = shear stress applied by pad on node 3

u = control force applied at node 3

Formulation of Equation of Motion

The formulation follows like any other finite element formulation again with the added time-dependent modulus as in problem 1. The basic equation of motion for an element is again

$$\tilde{m}\ddot{\vec{d}} + \tilde{k}\vec{d} = \vec{r} \tag{39}$$

From Cook the elastic rod element mass and stiffness matrices are

$$\tilde{m} = \frac{\rho AL}{6}\begin{bmatrix} 2 & 1 \\ 1 & 2 \end{bmatrix}$$

$$\tilde{k} = \frac{AE}{L}\begin{bmatrix} 1 & -1 \\ -1 & 1 \end{bmatrix}$$

The derivation of the general equation of motion by summation of forces on nodes is important to review here, in order to understand the inclusion of the shear force boundary condition in $\vec{r}$. Consider node 3, shown in Figure 9.

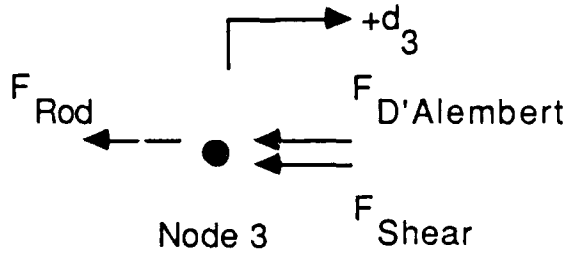

Figure 9. Free Body Diagram of Node 3 in Example 2

A positive displacement of the node is assumed to stretch the rod, like a spring, so the force on the node is in the negative direction. Furthermore, the rod mass is lumped on the node, so there is inertia. This creates the D'Alembert's force resisting the node motion. Finally, the shear force created by the shear pad is assumed to be a nodal point load. It too resists the positive displacement of node 3. Hence, the equation of motion for node 3 is

$$-\tilde{m}_3\ddot{\vec{d}}_3 - \tilde{k}_3\vec{d}_3 - A_c\vec{\tau} = \vec{0}$$

or

$$\tilde{m}_3\ddot{\vec{d}}_3 + \tilde{k}_3\vec{d}_3 + A_c\vec{\tau} = \vec{0}$$

Of course, node 2 does not have the shear force, so its equation is

$$\tilde{m}_2\ddot{\vec{d}}_2 + \tilde{k}_2\vec{d}_2 = \vec{0}$$

The derivation of the shear stress, τ, equation can be seen from Figure 10.

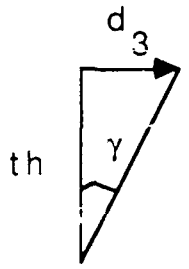

Figure 10. Diagram for Shear Force Equation Derivation

For small d_3 compared to th. the small angle approximation for the

shear strain, γ, applies, i.e. $\gamma \approx \tan \gamma = d_3/th$, and $\tau = G(t)\,\gamma = G(t)d_3/th$. This stress is applied over the contact area, A_c. Therefore, assembling the matrices and applying the boundary conditions gives the elastic system equation of motion. Taking the Laplace transform of the system and applying the correspondence principle to the shear modulus in the shear pad force gives

$$s^2 \tilde{M}\,\vec{D}(s) + \tilde{K}_e\,\vec{D}(s) = -G(s)\tilde{K'}_v\,\vec{D}(s) + \vec{U}(s) \qquad (60)$$

where

$$\vec{D}(s) = \begin{Bmatrix} D_2(s) \\ D_3(s) \end{Bmatrix}$$

$$\vec{U}(s) = \begin{Bmatrix} 0 \\ U(s) \end{Bmatrix}$$

$$\tilde{M} = \frac{\rho AL}{6}\begin{bmatrix} 4 & 1 \\ 1 & 2 \end{bmatrix}$$

$$\tilde{K}_e = \frac{AE}{L}\begin{bmatrix} 2 & -1 \\ -1 & 1 \end{bmatrix}$$

$$\tilde{K'}_v = \frac{A_c}{th}\begin{bmatrix} 0 & 0 \\ 0 & 1 \end{bmatrix}$$

where the d_i values are displacements of the ith node. The displacement d_1 was eliminated by the zero displacement boundary condition. $\tilde{M}$ is the assembled mass matrix, $\tilde{K}_e$ is the assembled matrix of stiffness corresponding to elastic elements (only the rods in this problem), and $G(t)\tilde{K'}_v$ is the assembled matrix of stiffness

due to viscoelastic elements (the shear pad). Using the value of G(s), the system equation of motion (EOM) is

$$\left[\tilde{M}\, s^2 + G_1 \tilde{K'}_v\, s^{1/2} + \left(G_0 \tilde{K'}_v + \tilde{K}_e\right) \right] \vec{D}(s) = \vec{U}(s) \quad \text{(EOM)} \tag{61}$$

Values for the matrices in this problem are

$$\tilde{M} = 0.04660 \begin{bmatrix} 4 & 1 \\ 1 & 2 \end{bmatrix} \text{kg}$$

$$\tilde{K}_e = 6.894 \times 10^6 \begin{bmatrix} 2 & -1 \\ -1 & 1 \end{bmatrix} \text{N/m}$$

$$G_0 \tilde{K'}_v = 7600 \begin{bmatrix} 0 & 0 \\ 0 & 1 \end{bmatrix} \text{N/m}$$

$$G_1 \tilde{K'}_v = 2950 \begin{bmatrix} 0 & 0 \\ 0 & 1 \end{bmatrix} \text{N-sec}^{1/2}\text{/m}$$

Open Loop Response

The eigenvalue problem is once again set up in the $s^{1/2}$-plane by defining $\lambda = s^{1/2}$, where λ_j and $\vec{\phi}_j$ are the jth eigenvalue and eigenvector. This gives

$$\left[\tilde{M}\, \lambda_j^4 + G_1 \tilde{K'}_v\, \lambda_j + \left(G_0 \tilde{K'}_v + \tilde{K}_e\right) \right] \vec{\phi}_j(s) = \vec{0} \tag{62}$$

which can be solved by the iteration scheme process described in Example 1. The first four eigenvalues and eigenvectors are shown in Table IV.

Table IV. First Four Open Loop Eigenvalue and Eigenvectors, Example 2

Eigenvalue	Eigenvector
$44.7541 \pm 45.4687i$	$\begin{Bmatrix} 0.7162 \pm 0.0088i \\ 1.0000 \end{Bmatrix}$
$-44.7542 \pm 44.0099i$	$\begin{Bmatrix} 0.6990 \pm 0.0084i \\ 1.0000 \end{Bmatrix}$

1/2-Order System Formulation

The expansion into the 1/2-fractional state space follows from the first example:

$$s^{1/2}\begin{bmatrix} \tilde{0} & \tilde{0} & \tilde{0} & \tilde{M} \\ \tilde{0} & \tilde{0} & \tilde{M} & \tilde{0} \\ \tilde{0} & \tilde{M} & \tilde{0} & \tilde{0} \\ \tilde{M} & \tilde{0} & \tilde{0} & \tilde{K}_1 \end{bmatrix}\begin{Bmatrix} s^{3/2}\vec{D}(s) \\ s^{1}\vec{D}(s) \\ s^{1/2}\vec{D}(s) \\ \vec{D}(s) \end{Bmatrix} + \begin{bmatrix} \tilde{0} & \tilde{0} & -\tilde{M} & \tilde{0} \\ \tilde{0} & -\tilde{M} & \tilde{0} & \tilde{0} \\ -\tilde{M} & \tilde{0} & \tilde{0} & \tilde{0} \\ \tilde{0} & \tilde{0} & \tilde{0} & \tilde{K}_0 \end{bmatrix}\begin{Bmatrix} s^{3/2}\vec{D}(s) \\ s^{1}\vec{D}(s) \\ s^{1/2}\vec{D}(s) \\ \vec{D}(s) \end{Bmatrix}$$

$$= \begin{bmatrix} \vec{0} \\ \vec{0} \\ \vec{0} \\ \vec{1} \end{bmatrix} U(s) \qquad (63)$$

where

$$\tilde{K}_0 = G_0\tilde{K'}_v + \tilde{K}_e$$

$$\tilde{K}_1 = G_1\tilde{K'}_v$$

$$\vec{0} = \begin{Bmatrix} 0 \\ 0 \end{Bmatrix}$$

$$\vec{1} = \begin{Bmatrix} 0 \\ 1 \end{Bmatrix}$$

Again let the expanded state vector be denoted by an underscore, i.e. $\underline{\vec{D}}(s)$. Note that U(s) is a scalar, because there is only one control force in this example. This is rearranged to the appropriate $s^1\,{}^{/2}\underline{\vec{D}}(s) = \tilde{A}\,\underline{\vec{D}}(s) + \tilde{B}\,\vec{U}(s)$ form, where

$$\tilde{A} = -\begin{bmatrix} \tilde{0} & \tilde{0} & \tilde{0} & \tilde{M} \\ \tilde{0} & \tilde{0} & \tilde{M} & \tilde{0} \\ \tilde{0} & \tilde{M} & \tilde{0} & \tilde{0} \\ \tilde{M} & \tilde{0} & \tilde{0} & \tilde{K}_1 \end{bmatrix}^{-1} \begin{bmatrix} \tilde{0} & \tilde{0} & -\tilde{M} & \tilde{0} \\ \tilde{0} & -\tilde{M} & \tilde{0} & \tilde{0} \\ -\tilde{M} & \tilde{0} & \tilde{0} & \tilde{0} \\ \tilde{0} & \tilde{0} & \tilde{0} & \tilde{K}_0 \end{bmatrix} \qquad (64)$$

$$\tilde{B} = \begin{bmatrix} \tilde{0} & \tilde{0} & \tilde{0} & \tilde{M} \\ \tilde{0} & \tilde{0} & \tilde{M} & \tilde{0} \\ \tilde{0} & \tilde{M} & \tilde{0} & \tilde{0} \\ \tilde{M} & \tilde{0} & \tilde{0} & \tilde{K}_1 \end{bmatrix}^{-1} \begin{bmatrix} \vec{0} \\ \vec{0} \\ \vec{0} \\ \vec{I} \end{bmatrix} \qquad (65)$$

$$\vec{U}(s) = U(s)$$

To complete the system, it is assumed that all states are outputs and that there is no feedforward to the output, i.e.

$$\vec{Y}(s) = \tilde{C}\,\underline{\vec{D}}(s) + \tilde{D}U(s) \qquad (66)$$

where

$\tilde{C}$ = 8 x 8 identity matrix
$\tilde{D}$ = 8 x 1 null (zero) matrix

Open Loop Poles Via MATRIXx

The above system reduces to the eigenvalue problem for open loop poles when the control vector, U(s), is set to zero. The eigenvalues of the A matrix are then the open loop poles. The first

eight eigenvalues are found by using the EIG function on $\tilde{A}$. These are shown in Table V with the closed loop poles. Having already found the first four by the iteration solution of the EOM, the second set of four can be identified. Notice that the first four are the same as found by the iteration method. Unfortunately, the mode shapes (eigenvectors) for the second set must be found by modifying the iterative solution of the EOM. The poles are shown graphically in Figure 11.

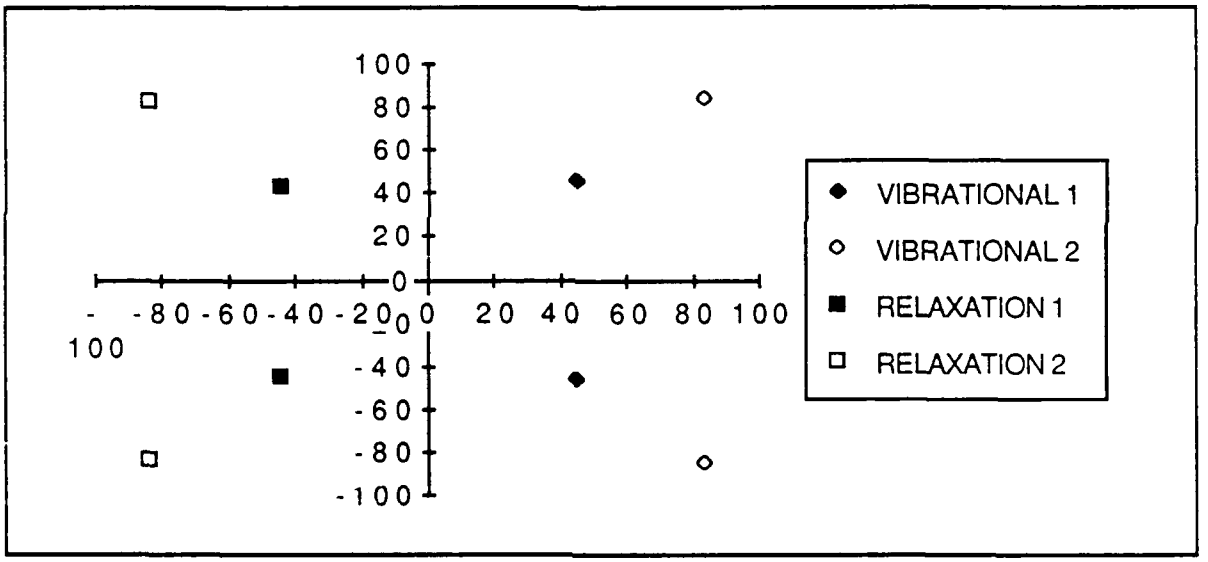

Figure 11. Example 2 Open Loop Poles for Both Vibrational and Relaxation Modes 1 and 2.

Closed Loop Poles Via MATRIX$_X$

The system is posed in the appropriate form for the Riccati equation solver: $\dot{\vec{D}}(t) = \tilde{A}^2 \vec{D}(t) + \tilde{A}\tilde{B}\, u(t)$. There are two weighting

matrices, because two cases are studied to show the effect of varying weights. This is also required to get a significant change in the pole locations - an example of the usefulness and arbitrariness of weighting to get a desired pole structure. The inputs for the Riccati function are

$$\tilde{S} = \begin{bmatrix} \tilde{A}^2 & \tilde{A}\tilde{B} \\ \tilde{C} & \tilde{D} \end{bmatrix}$$

$$\widetilde{RQ_1} = \begin{bmatrix} \tilde{0} & \tilde{0} & \tilde{0} & \tilde{0} & 0 \\ \tilde{0} & 10^6\tilde{I} & \tilde{0} & \tilde{0} & 0 \\ \tilde{0} & \tilde{0} & \tilde{0} & \tilde{0} & 0 \\ \tilde{0} & \tilde{0} & \tilde{0} & 10^6\tilde{I} & 0 \\ 0 & 0 & 0 & 0 & 1 \end{bmatrix}$$

$$\widetilde{RQ_2} = \begin{bmatrix} \tilde{0} & \tilde{0} & \tilde{0} & \tilde{0} & 0 \\ \tilde{0} & 10^9\tilde{I} & \tilde{0} & \tilde{0} & 0 \\ \tilde{0} & \tilde{0} & \tilde{0} & \tilde{0} & 0 \\ \tilde{0} & \tilde{0} & \tilde{0} & 10^9\tilde{I} & 0 \\ 0 & 0 & 0 & 0 & 1 \end{bmatrix}$$

NS = 8

MATRIX$_X$ then gives $\widetilde{KC_1}$ for $\widetilde{RQ_1}$:

$$\widetilde{KC_1} =$$

[-0.3709 -0.4680 14.986 1205.8 731.18 -3083.4 -3.1086D+06 1.5543D+06]

and the eigenvalues of the system, $s^{1/2}\vec{D}(s) = \left(\tilde{A} - \tilde{B}\widetilde{KC_1}\right)\vec{D}(s)$, are found by applying EIG() to $\left(\tilde{A} - \tilde{B}\widetilde{KC_1}\right)$. The mode to which each closed loop pole corresponds is determined by marching through

increasing feedback gain and observing the evolution of the poles from the open loop ones. The poles are shown in Table V.

MATRIX$_X$ gives $\widetilde{KC}_2$ for $\widetilde{RQ}_2$:

$$\widetilde{KC}_2 =$$

[-0.3667 -0.4311 3376.1 33925 1937 -3293 -2.6028D+08 1.3014D+08]

The corresponding eigenvalues are also shown in Table V.

Table V. $s^{1/2}$-Plane Open and Closed Loop Poles for Example 2

Open Loop	Closed Case 1	Closed Case 2
44.7541 ± 45.4687i	29.1442 ± 59.8026i	2.10 ± 631.92i
-44.7542 ± 44.0099i	-26.8325 ± 58.4049i	-0.01 ± 9.89i
83.6001 ± 84.0417i	64.9435 ± 95.0618i	54.06 ± 77.67i
-83.6000 ± 83.1657i	-64.9542 ± 93.3355i	-54.08 ± 77.71i

The closed loop poles are shown in Figures 12 and 13.

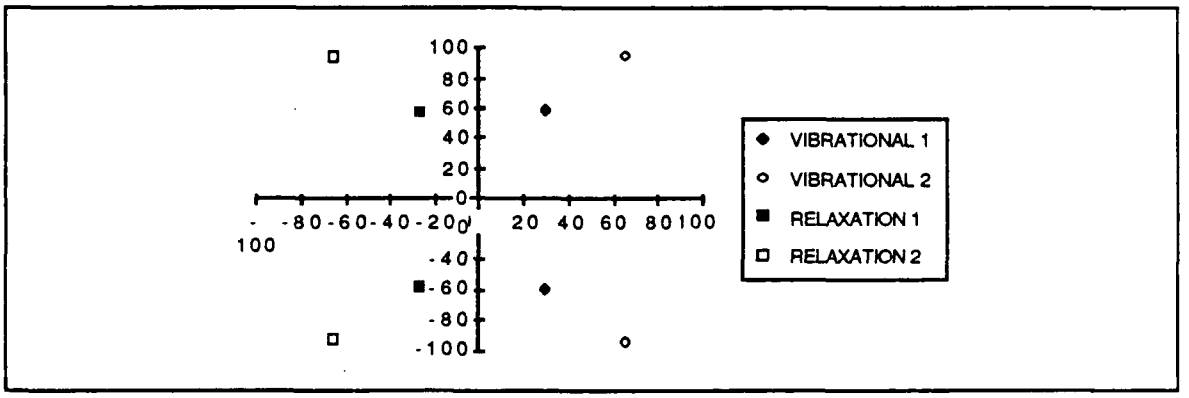

Figure 12. Example 2 Case A Closed Loop Poles for Both Vibrational and Relaxation Modes 1 and 2.

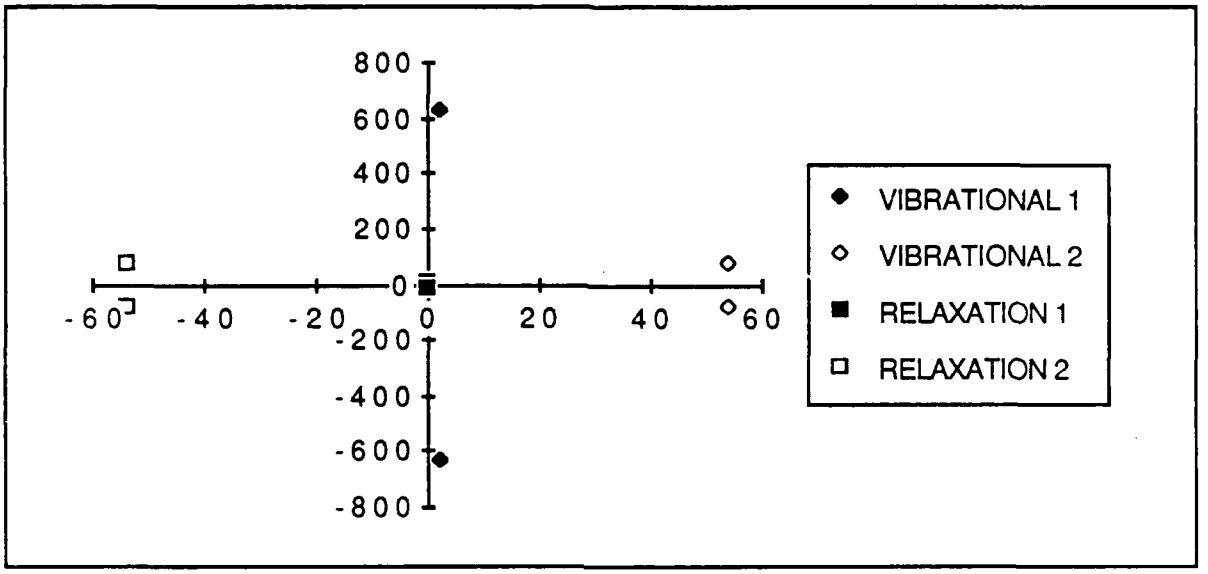

Figure 13. Example 2 Case B Closed Loop Poles for Both Vibrational and Relaxational Modes 1 and 2.

Comparison of Open and Closed Loop Poles

The stability measures based on the $s^{1/2}$-plane open and closed looo poles are shown in Table VI, and the oscillatory motion parameters are shown in Table VII.

Table VI. Stability Measures for Example 2

Mode	Re(O)	Re(C)	Re(O)-Re(C)	Open l/R	Closed l/R
Case 1					
1	44.7541	29.1442	15.6099	1.0160	2.0520
	-44.7542	-26.8325	-17.9217	0.9834	2.1766
2	83.6001	64.9435	18.6566	1.0053	1.4638
	-83.6000	-64.9542	-18.6458	0.9948	1.4369
Case 2					
1	44.7541	2.1	42.6541	1.0160	300.91
	-44.7542	-0.01	-44.7442	0.9834	989.00
2	83.6001	54.06	29.5401	1.0053	1.4367
	-83.6000	-54.08	-29.5200	0.9948	1.4369

Table VII. Example 2 Oscillatory Motion Parameters

EV $s^{1/2}$	EV s^1	ζ	ω_n	ω_d
Open Loop				
44.7541 ± 45.4687i	-64.473 ± 4069.8i	0.0158	4080.6	4069
83.6001 ± 84.0417i	-74.031 ± 14052.7i	0.0053	14053.3	14052
Closed Loop Case 1				
29.1442 ± 59.8026i	-2727.0 ± 3485.8i	0.6162	4425.7	3485
64.9435 ± 95.0618i	-4819.1 ± 12342.3i	0.3637	13249.4	12342
Closed Loop Case 2				
2.1000 ± 631.92i	-399318 ± 2654.1i	≈1.0000	399318	2654
54.0600 ± 77.67i	-3110.1 ± 8397.7i	0.3473	8955.1	8397

Both closed loop cases show improvement in stability over the open loop case. Mode one damping ratio increases from 0.0158 to 0.6162 and approximately 1.0. Its natural frequency also increases from 4080.6 rad/sec to 4425.7 rad/sec and 399318 rad/sec, in cases A

and B respectively. Although the damping ratio increases for Mode 2, its natural frequency decreases. Interestingly, the damped frequency for both modes decreases. Therefore, resonance occurs at lower frequencies but at a reduced magnification factor, $|G(i\omega)| = \left\{\left[1 - (\omega/\omega_n)^2\right]^2 + (2\zeta\omega/\omega_n)^2\right\}^{-1/2}$. In fact, for case 2 the system is approximately critically damped, so there would be no resonance for that mode. Mode 2, interestingly, has a better damped response in case 1 than in case 2 because of a lower $G(i\omega)$ and faster decrease in the amplitude envelope. At resonance the larger ζ results in a lower magnification factor, and the larger $\zeta\omega_n$ product causes the amplitude to die faster ($e^{-\zeta\omega_n t}$). Furthermore, case 1 has a better separation of resonance frequencies than case 2, but neither has better separation than the open loop. Evidently, minimizing the performance index does not mean that all stability parameters will improve. It is possible that controlling mode 1 is having an effect on mode 2 such that the latter is being destabilized. Nevertheless, even at resonance the system is displaying reduced motion.

Closed loop cases 1 and 2 demonstrate how weighting can significantly change results. In the modified example 1 equal weighting was sufficient to create a significant difference in the pole structure, while here in example 2 weights of 10^6 and 10^9 were required to make significant changes. Hence, the guideline for weighting is the desired pole structure at the end. Furthermore, various combinations of weights can result in similar pole structures. For example, weighting velocity at 10^6 and control at

10^{-3} yields results similar to weighting velocity at 10^{9}. For a guideline on weighting remember from example 1 that the velocity and derivative of order 3/2 in feedback have strong effects on poles, while the derivatives of lesser order have much less effect. Therefore, to make a significant change in pole location, one should weight the velocity or derivative of order 3/2 ; while weighting position should only make small changes to the pole structure. Since the control vector becomes full state feedback, weighting it has mixed effects, because it includes all derivatives. However, example 2 results indicate that the conrol vector effect is dominated by the higher order derivatives, which allowed weighting velocity at 10^{6} and control at 10^{-3} to yield results similar to weighting velocity at 10^{9}.

V. Conclusions

Quadratic control theory can be used to find an optimal feedback control law at steady state conditions for a structure incorporating a fractional calculus model of viscoelasticity. Following linear regulator control theory, it has been shown that under large time conditions the optimal control law is linear state feedback, assuming an optimal time-varying gain matrix, K, which is asymptotically constant for large time, for the minimized performance index. A Riccati equation is created, such that a fractional derivative system of order 1/n (n an integer) can be represented by an equivalent first-order system in Riccati equation solving routines. Therefore, current tools can be used to easily solve problems of this kind. By expanding the structure's equation of motion into a fractional state-space system, the control theory can be applied to structures incorporating both passive and active damping. This has been illustrated in two example problems.

The theory is limited to optimal gain matrices which are asymptotically constant for large time. The optimal control , as determined by linear regulator theory, is asymptotically linear feedback as time tends to infinity. The evaluation of the Hamilton-Jacobi-Bellman equation cannot produce a Riccati equation in general time for a time-varying optimal gain because of coupling of the gain matrix and the state vector due to fractional derivatives acting on the control vector. Only when time tends to infinity can

these derivatives be neglected. Then the optimal gain matrix can be decoupled from the state vector, and an algebraic Riccati equation can be identified for time large and for an optimal gain matrix which is asymptotically constant for large time.

VI. Recommendation for Further Work

The next step is to test the theory by experiment. Captain Kevin Klonoski's thesis research (16) has developed a prototype sensor for fractional derivative motion, and a design useful for experimentation should be developed. Response of a simple beam structure should then be predicted using the theory and compared to experimental results using such a sensor to feed back the fractional state vectors. This will also require the development of a discrete-time model and theory, if digital control is to be used. Thus, verification requires:

1. Design of a fractional derivative sensor suitable for experiment instrumentation;

2. Development of a discrete-time version of the theory in order to apply digital control (if desired);

3. Comparison of the predictions with experimental data for a simple system.

Further theoretical research could examine the effect of optimal performance index forms other than that used in linear regulatory theory. There is evidence that time delay in feedback loops can cause exponential instability. Hence, further research could study the effect of time-delayed feedback on systems using this theory.

Another possible area of interest is the investigation of the effect of this theory on modes over a large range of frequencies. I

have only worked with the first and second modes and there are significant differences in results between the two example problems. Examination of the effect on a larger range of modes and comparison with physical theory on how those higher modes should be effected could give insight to the accuracy and utility of this control model.

Appendix A: Regularly-Varying Functions

The presentation in this appendix is excerpted with minor changes from Warhola (26).

"Regularly-varying" functions are those functions, f(t), for which f(ct)/f(t) approaches a *finite non-zero limit* as $t \rightarrow \infty$; *for* any such function, the limit is necessarily of the form c^p as a function of the parameter c, with $-\infty < p < \infty$ (10). In this limit, f has the asymptotic behavior:

$$f(ct) \sim c^p f(t), \quad t \rightarrow \infty \tag{A.1}$$

For such a function, the notation P(f) = p indicates that p is the "power" of f.

If Eq (A.1) *holds with* p = 0, *the function is "slowly-varying."* To suggest a logarithm, L(t) is used to denote any otherwise unspecified slowly-varying function. Then

$$L(ct) \sim L(t), \quad t \rightarrow \infty \tag{A.2}$$

Any regularly-varying function f(t) can be expressed in the form

$$f(t) = L(t)\ t^p \tag{A.3}$$

For many purposes, L can be treated as if it were a constant, even though it may converge to *zero* or *diverge to infinity*. *For example*, powers and products of regularly-varying functions are also regularly-varying, with the obvious exponents. In particular, any function which approaches a non-zero constant value is slowly-varying.

If the slope on a log-log graph of a differentiable function, f(t), approaches a constant, p, for $t \to \infty$,

$$d(\ln f(t))/d(\ln t) = tf'(t)/f(t) \to p, \quad t \to \infty \tag{A.4}$$

then f is regularly-varying with P(f) = p. Additionally, f' is also regularly-varying (unless f is merely slowly-varying), with P(f') = p-1:

$$f'(t) \sim p\, f(t)/t \ , \quad p \neq 0 \ , \ t \to \infty \tag{A.5a}$$

$$f'(t) = o(\, f(t)/t \,), \quad p = 0 \ , \ t \to \infty \tag{A.5b}$$

The exception for p = 0 occurs because when f is approaching a constant, f' may be approaching zero much faster than 1/t.

On the contrary, when f is regularly-varying, its indefinite integral F is always regularly-varying (10). When F diverges as $t \to \infty$,

$$F(t) = \int_0^t f(\tau)\, d\tau \sim \frac{t\ f(t)}{p+1} \ , p = P(f) > -1 \ , \ t \to \infty \tag{A.6}$$

just as if f were actually a power. When p<-1 , the integral in Eq (A.6) approaches a constant and the tail of the integral is regularly-varying:

$$\int_t^\infty f(\tau)\, d\tau \sim \frac{t\ f(t)}{|p+1|} \ , p = P(f) < -1 \ , \ t \to \infty \tag{A.7}$$

The result analogous to Eq (A5.b) is

$$t\, f(t) = o(F) \quad , p = P(f) < -1 \ , \ t \to \infty \tag{A.8}$$

A useful result is added here for the convolution of two regularly-varying functions of a certain class. If f(t) and g(t) vanish for $t < 0$, and are regularly-varying at infinity with powers $P(f) = p > -1$ and $P(g) = q > -1$, then

$$\int_0^t f(t-\tau)\, g(\tau)\, d\tau \sim \frac{p!\, q!}{(p+q+1)!}\ t\, f(t) g(t) \ , \ p, q > -1 \ , \ t \to \infty \tag{A.9}$$

where

$$p! = \int_0^\infty t^p\, e^{-t}\, dt \ , \ p > -1$$

Appendix B: 4BEAMEVS.EXC Listing

This is a listing of the MATRIX$_X$ command file (14:7-3 - 7-6) called 4BEAMEVS.EXC. This file determines the open loop eigenvalues and eigenvectors for the first mode of a fourth-order beam equation of motion which incorporates a fractional calculus model of viscoelasticity of order 1/2, i.e. the fractional derivatives are of order 1/2.

The file is interactive. The user must supply the assembled mass, elastic stiffness (K_0), and viscoelastic stiffness (K_1) matrices, as defined in Chapter IV. The user must also supply an initial guess of the eigenvalue and eigenvector. The iteration process is not automated, so the file will ask which of four possible roots should it follow. Choose one set of signs to follow at a time until the root converges within an acceptable error. Complete this four times to get all four eigenvalues and eigenvectors. Answer the query on which root to follow by RT(element number of proper root). The vector of roots is called RT, so RT(#) specifies a specific element.

The eigenvalues and eigenvectors are written to file EV.DAT as vector EVAL and matrix EVEC. Each column of EVEC is an eigenvector.

```
DISPLAY('EIGENVALUE/VECTOR SOLN FOR 4TH ORDER BEAM THEORY')
INQUIRE N 'ENTER NUMBER OF DOF'
INQUIRE M 'ENTER ASSEMBLED CONSISTENT MASS MATRIX'
INQUIRE K0 'ENTER ASSEMBLED K0 MATRIX'
INQUIRE K1 'ENTER ASSEMBLED K1 MATRIX'
```

```
E0K=K0;
E1K=K1;
INQUIRE L1 'ENTER INITIAL LAMBDA1 GUESS'
INQUIRE EV1 'ENTER INITIAL EIGENVECTOR1 GUESS'
K2=L1*E1K+E0K;
K2INV=INV(K2);
EV1ERR=1;
WHILE EV1ERR>5D-6,...
  LHS=K2INV*M*EV1;...
 LHSMAX=LHS(1);...
 FOR I=2:N, IF ABS(LHS(I))>ABS(LHSMAX), LHSMAX=LHS(I);END,END,...
 EVT=LHS/LHSMAX,...
  EV1ERR=ABS(EVT(1)-EV1(1));...
 FOR I=2:N,...
   IF EVT(I)<>EV1(I),...
     ERR=ABS(EVT(I)-EV1(I)),...
   IF ERR>EV1ERR,EV1ERR=ERR;END,...
  END,...
 END,...
 IF EV1ERR>5D-6, EV1=EVT;END,...
END
LHSMAX=LHSMAX
H=1/LHSMAX;
P=[1,0,0,0,H];
RTBASE=ROOTS(P)
FOR J=1:4,...
 L1=RTBASE(J);...
 CHOICE=0;...
 OLDRLERR=1;...
 OLDIMERR=1;...
 ITER=1,...
 WHILE CHOICE<1,...
   K2=L1*E1K+E0K;...
   K2INV=INV(K2);...
  EV1ERR=1;...
  WHILE EV1ERR>5D-6,...
     LHS=K2INV*M*EV1;...
    LHSMAX=LHS(1);...
     FOR I=2:N, IF ABS(LHS(I))>ABS(LHSMAX),
LHSMAX=LHS(I);END,END,...
    EVT=LHS/LHSMAX;...
     EV1ERR=ABS(EVT(1)-EV1(1));...
```

```
      FOR I=2:N,...
        IF EVT(I)<>EV1(I),...
          ERR=ABS(EVT(I)-EV1(I));...
        IF ERR>EV1ERR,EV1ERR=ERR;END,...
       END,...
      END,...
      IF EV1ERR>5D-6, EV1=EVT;END,...
    END,...
    LHSMAX=LHSMAX,...
    H=1/LHSMAX;...
     P=[1,0,0,0,H];...
    RT=ROOTS(P),...
    INQUIRE L1TEMP 'WHICH ROOT TO CONTINUE ON BRANCH?',...
    ERRTEST=L1TEMP-L1;...
    NEWRLERR=REAL(ERRTEST);...
    NEWIMERR=IMAG(ERRTEST);...
    DRLERR=NEWRLERR-OLDRLERR,...
    DIMERR=NEWIMERR-OLDIMERR,...
    INQUIRE CHOICE 'CONTINUE=0 STOP=1',...
    OLDRLERR=NEWRLERR;...
    OLDIMERR=NEWIMERR;...
    L1=L1TEMP,...
    ITER=ITER+1,...
  END,...
EVAL(J)=L1TEMP,...
FOR I=1:N, EVEC(I,J)=EV1(I),END,...
END
PRINT('EV.DAT',EVAL)
PRINT('EV.DAT',EVEC)
RETURN
```

Bibliography

1. Bagley, Ronald L. Applications of Generalized Derivatives to Viscoelasiticity. PhD dissertation. School of Engineering, Air Force Institute of Technology (AU), Wright-Patterson AFB OH, November 1979 (AD-A071726).

2. Bagley, R.L. and Torvik, P.J. "Fractional Calculus - A Different Approach to the Analysis of Viscoelastically Damped Structures," AIAA Journal, 21:741-748. (May 1983).

3. -----. "Fractional Calculus in the Transient Analysis of Viscoelatically Damped Structures," AIAA Journal, 23: 918-925 (June 1985).

4. -----. "A Generalized Derivative Model for an Elastomer Damper," Shock and Vibration Bulletin, 49: 135-143 (September 1979).

5. Christensen, R.M. Theory of Viscoelasticity: An Introduction. USA: Academic Press, Inc, 1971.

6. Churchill, Ruel V. Operational Mathematics (Third Edition). New York: McGraw-Hill, Inc, 1972.

7. Cook, Robert D. Concepts and Applications of Finite Element Analysis (Second Edition). New York: John Wiley and Sons, Inc, 1981.

8. Devereaux, Michele L. Improved Solution Techniques for the Eigenstructure of Fractional Order Systems. MS thesis. School of Engineering, Air Force Institute of Technology (AU), Wright-Patterson AFB OH, December 1988.

9. Ewing, George M. Calculus of Variations with Applications. USA: W.W. Norton and Company,Inc, 1969.

10. Feller, W. An Introduction to Probability Theory and its Applications, Vol II (Second Edition). New York: John Wiley and Sons, Inc, 1971.

11. Forray, Marvin J. Variational Calculus in Science and Engineering. USA: McGraw-Hill Book Company, 1968.

12. Hannsgen, Kenneth B., et al. "Effectiveness and Robustness with Respect to Time Delays of Boundary Feedback Stabilization in One-Dimensional Viscoelasticity," to be published in SIAM Journal of Control and Optimization.

13. Hestenes, Magnus R. Calculus of Variations and Optimal Control Theory. USA: John Wiley and Sons, Inc, 1966.

14. Integrated Systems, Inc. MATRIX$_X$ User Manual (Version 6.0). Palo Alto CA: Integrated Systems, Inc, 1986.

15. Kirk, Donald E. Optimal Contol Theory: An Introdution. USA: Prentice-Hall, Inc 1979.

16. Klonoski, Kevin D. Fractional Order Feedback for Viscoelastic Systems. MS thesis. School of Engineering, Air Force Institute of Technology (AU), Wright-Patterson AFB OH, to appear.

17. Kreyszig, Erwin. Advanced Engineering Mathematics. USA: John Wiley and Sons, Inc, 1983.

18. Meirovitch, Leonard. Analytical Methods in Vibrations. New York: MacMillan Publishing Co, Inc, 1967.

19. -----. Elements of Vibration Analysis (Second Edition). New York: McGraw-Hill, Inc, 1986.

20. Nutting, P.G. "A New Generalized Law of Deformation," Journal of the Franklin Institute, 191: 679-685 (1921).

21. Oldham, Keith B. and Spanier, Jerome. The Fractional Calculus. USA: Academic Press, Inc, 1974.

22. Reid, J. Gary. Linear System Fundamentals. New York: Mc Graw-Hill, Inc, 1983.

23. Roff, W.J. Fibers, Plastics, and Rubbers: A Handbook of Common Polymers. New York: Academic Press, Inc, 1956.

24. Skaar, Steven B. , et al. "Stability of Viscoelasitic Control Systems," IEEE Transactions on Automatic Control, 33: 348-357 (April 1988).

25. Torvik, P.J. and Bagley, R.L. "Fractional Derivatives in the Description of Damping Materials and Phenomena," The Role of Damping in Vibration and Noise Control, 5:125-135.

26. Warhola, G. T. Steady Waves in a Nonlinear Theory of Viscoelasticity. PhD dissertation. Brown University, Providence RI, 1988.

27. ----- "Asymptotic Behavior of Certain Fractional Derivatives and the Existence of State Vector Solutions": to appear.

Vita

Captain Richard N. Walker [redacted]

proceeded to the University of Colorado, Boulder, to study aerospace engineering. In May 1983 he graduated with a B.S. in aerospace engineering and as a distinguished ROTC graduate, accepted two bars of gold and a regular commission in the United States Air Force. He got his first choice of assignments and joined the Air Force Rocket Propulsion Laboratory (now the Astronautics Laboratory) at Edwards AFB, in September 1983. For four years Captain Walker fulfilled a childhood dream of hobknobbing with rocket scientists as he managed research and test programs for ICBM and Launch Vehicle solid propellant propulsion systems. After four years on "the Rock" in the middle of no place, MPC again gave him his choice of assignments in 1987 and he was bound for Dayton, OH, and AFIT to seek a Masters Degree in Astronautical Engineering. Capt Walker's next assignment is a PhD program in aeronautical/astronautical structures at Stanford University. His follow-on assignment is to teach at AFIT.

[redacted]

UNCLASSIFIED
SECURITY CLASSIFICATION OF THIS PAGE

REPORT DOCUMENTATION PAGE

Form Approved
OMB No. 0704-0188

1a. REPORT SECURITY CLASSIFICATION UNCLASSIFIED	1b. RESTRICTIVE MARKINGS
2a. SECURITY CLASSIFICATION AUTHORITY	3. DISTRIBUTION/AVAILABILITY OF REPORT Approved for public release; distribution unlimited
2b. DECLASSIFICATION/DOWNGRADING SCHEDULE	
4. PERFORMING ORGANIZATION REPORT NUMBER(S) AFIT/GA/AA/88D-12	5. MONITORING ORGANIZATION REPORT NUMBER(S)
6a. NAME OF PERFORMING ORGANIZATION School of Engineering 6b. OFFICE SYMBOL (If applicable) AFIT/ENY	7a. NAME OF MONITORING ORGANIZATION
6c. ADDRESS (City, State, and ZIP Code) Air Force Institute of Technology (AU) Wright-Patterson AFB, OH 45433-6583	7b. ADDRESS (City, State, and ZIP Code)
8a. NAME OF FUNDING/SPONSORING ORGANIZATION Vehicle Systems Division 8b. OFFICE SYMBOL (If applicable) AFAL/VSSS	9. PROCUREMENT INSTRUMENT IDENTIFICATION NUMBER
8c. ADDRESS (City, State, and ZIP Code) Air Force Astronautics Laboratory Edwards AFB, CA 93523-5000	10. SOURCE OF FUNDING NUMBERS PROGRAM ELEMENT NO. / PROJECT NO. / TASK NO / WORK UNIT ACCESSION NO.

11. TITLE (Include Security Classification)
(U) QUADRATIC OPTIMAL CONTROL THEORY FOR VISCOELASTICALLY DAMPED STRUCTURES USING A FRACTIONAL CALCULUS MODEL

12. PERSONAL AUTHOR(S)
Richard N. Walker, Capt, USAF

13a. TYPE OF REPORT	13b. TIME COVERED	14. DATE OF REPORT (Year, Month, Day)	15. PAGE COUNT
MS Thesis	FROM _____ TO _____	1988 December	106

16. SUPPLEMENTARY NOTATION

17. COSATI CODES			18. SUBJECT TERMS (Continue on reverse if necessary and identify by block number)
FIELD	GROUP	SUB-GROUP	Control, control theory, elastic properties/viscoelasticity
20	04		
12	09		

19. ABSTRACT (Continue on reverse if necessary and identify by block number)

Thesis Advisor: Lt Col Ronald Bagley
Associate Professor of Mechanics

ABSTRACT ON BACK

12 Jan 1989

20. DISTRIBUTION/AVAILABILITY OF ABSTRACT	21. ABSTRACT SECURITY CLASSIFICATION
☒ UNCLASSIFIED/UNLIMITED ☐ SAME AS RPT ☐ DTIC USERS	UNCLASSIFIED
22a. NAME OF RESPONSIBLE INDIVIDUAL Lt Col Ronald Bagley	22b. TELEPHONE (Include Area Code) (513)255-3517 22c. OFFICE SYMBOL AFIT/ENY

DD Form 1473, JUN 86 *Previous editions are obsolete.*

SECURITY CLASSIFICATION OF THIS PAGE
UNCLASSIFIED

Block 19 Abstract

The objective of this thesis is to develop a control law for structures incorporating both passive damping via viscoelastic materials modelled by a fractional calculus stress-strain law and active damping by applied forces and torques. To achieve this, quadratic optimal control theory is modified to accomodate systems with fractional derivatives in the state vector. Specifically, linear regulator theory is modified.

The approach requires expanding the structure's equation of motion into a fractional state-space system of order 1/n, where n is an integer based on the viscoelastic damping material constitutive law. This approach restricts the theory to materials which have rational, fractional derivatives in their constitutive laws. An equivalent first-order system is then formed and used to derive the optimal control theory in linear regulator problems. The quadratic performance index used in linear regulator theory is used, and equations similar to those derived for linear regulator problems using first-order systems are developed. The optimal control law is asymptotically linear feedback of the state vector for time large. An equation which defines the optimal gain matrix for the feedback is derived and is asymptotically an algebraic Riccati equation for long time and for gain matrices which are asymptotically constant for large time. Since an algebraic Riccati equation can be defined, current solving routines can determine the asymptotically constant optimal gain matrix for large time for the fractional state-space system.

In the general time case, no Riccati equation can be derived because of coupling between the optimal gain matrix and the state vector due to fractional derivatives of the control vector. Only when gain matrices are asymptotically constant for time large and time is large, do they uncouple.

The theory is illustrated by two examples. A simply-supported viscoelastic beam with controllers illustrates the solution process in Example 1. The beam example incorporates the fractional calculus viscoelastic behavior in a structure element, while an axially deforming rod in Example 2 incorporates the behavior through a viscoelastic shear force applied at a node by a damping pad. The example equations of motion are numerically solved using the commercially-available control analysis software package called MATRIX_X.